



COMMISSION OF THE
EUROPEAN COMMUNITIES



Equitable Testing and Evaluation of Marine Energy Extraction Devices in terms of Performance, Cost and Environmental Impact

Grant agreement number: 213380



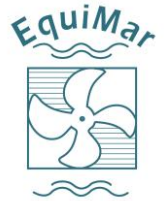
Deliverable D2.5 Tidal Model Intercomparison

Grant Agreement number: 213380

Project acronym: EQUIMAR

Project title: Equitable Testing and Evaluation of Marine Energy Extraction Devices in terms of Performance, Cost and Environmental Impact

Deliverable D2.5



Tidal Model Intercomparison

Christelle Herry and Françoise Girard

Actimar, France

John Lawrence

EMEC, UK

Vengatesan Venugopal and Thomas Davey

The University of Edinburgh, UK

March 2011

Summary

This report examines the application of a number of numerical tidal current models to the process of quantifying the resource at a specific site. The results and analysis presented are intended to give practical insight to the modelling processes involved in a site specific resource assessment. Variations between the models are examined and discussed.



CONTENTS

1	INTRODUCTION.....	1—1
1.1	MODEL INTERCOMPARISON FOR RESOURCE ASSESSMENT.....	1—1
1.1.1	<i>Scope of this Report.....</i>	<i>1—1</i>
1.1.2	<i>Numerical Models for Resource Assessment.....</i>	<i>1—1</i>
1.2	RESOURCE ASSESSMENT.....	1—1
1.2.1	<i>Resource Characterisation.....</i>	<i>1—1</i>
1.2.2	<i>Site Assessment.....</i>	<i>1—1</i>
2	MODEL OVERVIEW, REQUIREMENTS AND INPUTS	2—2
2.1	INTRODUCTION	2—2
2.2	TIDAL MODELLING OVERVIEW	2—2
2.2.1	<i>Governing equations</i>	<i>2—2</i>
2.2.2	<i>Numerical resolution and Computational Grids</i>	<i>2—3</i>
2.3	TIDAL MODELS	2—4
2.3.1	TELEMAC-2D.....	2—4
2.3.1.1	Computational Grid.....	2—4
2.3.1.2	Modelled Processes.....	2—4
2.3.1.3	Input Data.....	2—5
3	MODEL INTERCOMPARISON AT ORKNEY, UK.....	3—6
3.1	SITE SUMMARY	3—6
3.1.1	<i>Location.....</i>	<i>3—6</i>
3.1.2	<i>Bathymetry</i>	<i>3—6</i>
3.2	CALIBRATION AND VALIDATION DATA.....	3—7
3.2.1	<i>Presentation of hydrodynamic validation data</i>	<i>3—7</i>
3.2.2	<i>Presentation of meteorological forcing data.....</i>	<i>3—8</i>
3.3	TELEMAC-2D MODELLING	3—10
3.3.1	<i>Model Setup.....</i>	<i>3—10</i>
3.3.2	<i>Model Output.....</i>	<i>3—11</i>
3.3.3	<i>Adjustment of bottom friction coefficient.....</i>	<i>3—17</i>
3.3.4	<i>Influence of meteorological forcing</i>	<i>3—18</i>
3.4	MIKE21 MODELLING.....	3—21
3.4.1	<i>Model Setup.....</i>	<i>3—21</i>
3.4.2	<i>Model Output.....</i>	<i>3—23</i>
4	DISCUSSION	4—35

1 INTRODUCTION

1.1 MODEL INTERCOMPARISON FOR RESOURCE ASSESSMENT

1.1.1 Scope of this Report

This report examines the practicalities of applying a numerical model to characterise a potential tidal energy site. A selection of models are used to analyse a common dataset and provide insight into the comparability and performance of these models.

Document D2.3 (*Application of Numerical Models*) gives guidance on the setup, inputs and calibration/validation of numerical models. Elements of D2.3 are reproduced here for the purposes of background and clarity.

1.1.2 Numerical Models for Resource Assessment

Numerical models potentially play several important roles in the assessment of the marine energy resource. For geographical level *Resource Characterisation* a model may be deployed to provide data over a wide area for a statistically significant period of time. This combination of wide spatial and long temporal coverage is generally not feasible by direct measurement. Point measurement devices (e.g. ADCP) require multiple deployments to provide useful spatial information and long measurement programmes are not economical.

Having identified potentially exploitable sites with the aid of the resource characterisation process a more detailed *Site Assessment* must be conducted. This process aims to provide detailed spatial information sufficient for determining the placement of individual devices along with an understanding of the temporal variations expected over the life of the project.

Tidal current measurements, as with wave measurements, tend to be limited to point measurements with limited durations. Analysis of the harmonic components allows long term prediction of currents at geographical level. Numerical modelling aims to provide detailed spatial and temporal information accounting for local bathymetry and coastline influences.

In addition to the long term predictions numerical modelling may also play a role in short term forecasting. The problems associated with the variable nature of the resource (particularly the supply of electricity to the grid) may be mitigated in part if the output can be predicted several days in advance at a particular marine energy site. A calibrated numerical model, likely supported by on-site measurements, may be capable of providing short term forecasts based upon distant data from measurements or a global model.

1.2 RESOURCE ASSESSMENT

Marine energy resource assessments may be conducted to various levels of detail depending on the stage of a project or the end user. In particular assessments may be conducted to identify suitable geographic locations for deployment. Once suitable areas have been identified a detailed assessment will be necessary to characterise a particular site. These processes will be referred to as *Resource Characterisation* and *Site Assessment* in the outputs of the EquiMar project.

1.2.1 Resource Characterisation

Resource characterisation is normally carried out to establish suitable geographic locations for deployment, and has the following objectives:

- To ascertain the potential resource for energy production with an explicitly stated degree of uncertainty;
- To identify constraints on resource harvesting.

1.2.2 Site Assessment

Site assessment is normally carried out prior to deployment, to establish the detailed physical environment for a particular marine energy project, with the following objectives:

- To assess the energy production throughout the life of the project;
- To characterise the bathymetry of the site to an explicitly specified and appropriate resolution;
- To ascertain the spatial and temporal variation of the resource with an explicitly stated degree of uncertainty;
- To describe metocean conditions;
- To establish extreme (survivability) conditions with a defined return period;
- To identify potential interference between multiple devices at the site.

2 MODEL OVERVIEW, REQUIREMENTS AND INPUTS

2.1 INTRODUCTION

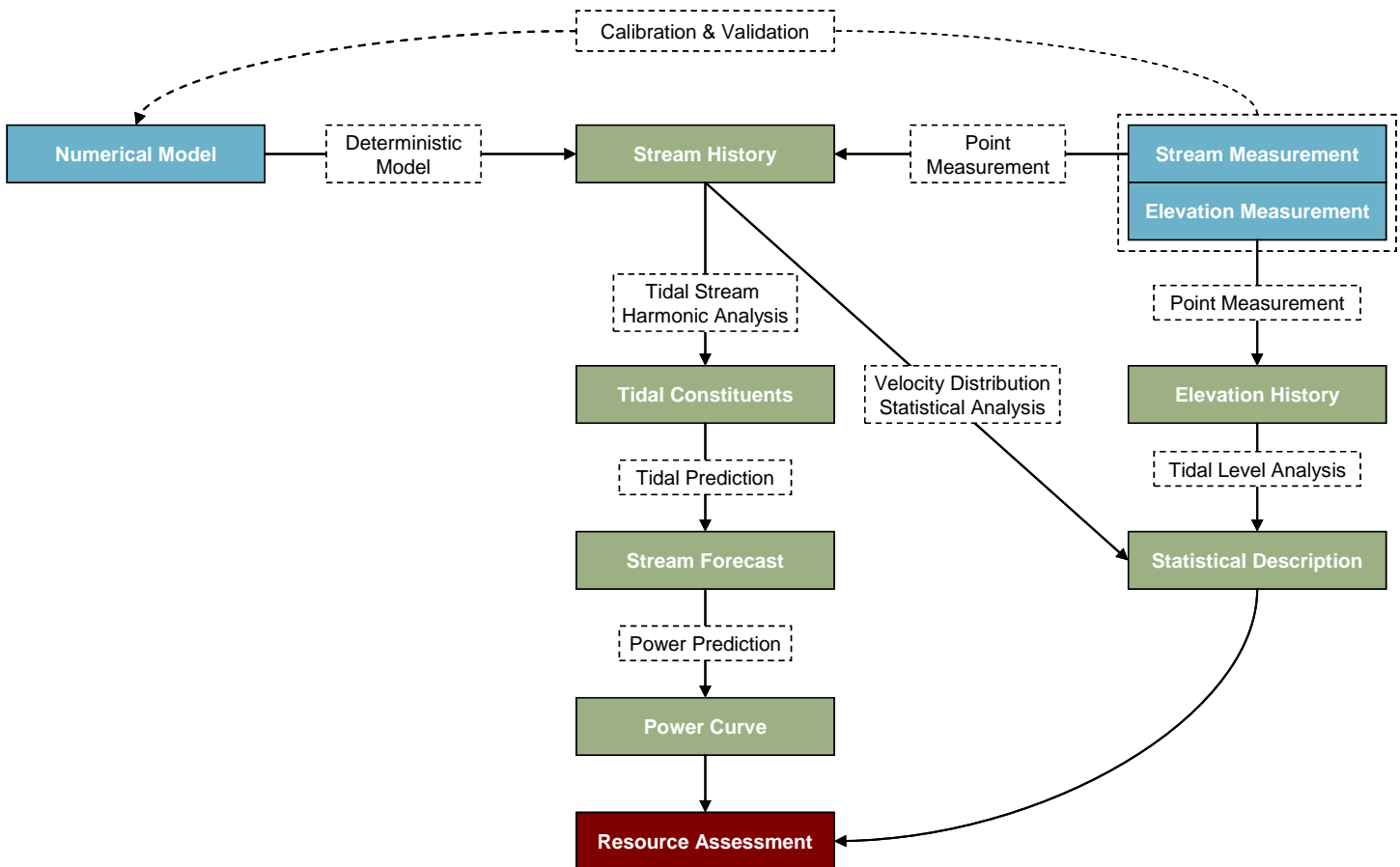


Figure 1 Schematic representation of possible tidal Resource Assessment procedures

The forces driving tidal motions are astronomic in nature and mainly governed by the relative positions of the Earth, Sun and Moon. The Newtonian theory of tides enables determination of the tide-generating forces on the ocean waters and is capable of explaining the existence of tides, including the harmonic periods governing the temporal variations in tidal behaviour. However, it cannot explain the local variations in amplitude caused by geographic effects. The presence of coastlines and depth variations modify the response of the oceanic waters to the astronomic tide-generating forces and the flow speed varies in both space and time.

Measurements may provide good information on water levels and currents but, when available, the information is usually based upon a limited point measurement (at one position and for a limited duration). Modelling provides an effective means of completing this information in time and space given knowledge of the local bathymetry.

The role of numerical models in resource assessment in relation to measurement techniques is illustrated graphically in Figure 1.

2.2 TIDAL MODELLING OVERVIEW

2.2.1 Governing equations

To compute sea level and currents, coastal hydrodynamic models solve the Navier-Stokes equations. Most of the time (for example for the models MARS3D, ROMS, MIKE) these equations are simplified using the following assumptions:

- Hydrostaticity: vertical motion is much smaller than horizontal motion
- Boussinesq approximation: the variation in density is neglected everywhere except in the buoyancy term

In 3 dimensions, these equations have to be completed by thermodynamic equations to model:

- The advection-diffusion of tracers particularly Temperature and Salinity
- The solar radiation flux and the surface ocean-atmosphere heat flux

When integrating along the vertical, the primitive equations can be simplified in a 2 dimension horizontal system called ‘‘Saint-Venant’’ system. This 2D model is most of the time an efficient mean to represent coastal propagation of tide and to estimate tidal level ζ and barotropic currents (u,v) in shallow water.

Equation of motion:

$$\begin{aligned} \frac{\partial u}{\partial t} + u \frac{\partial u}{\partial x} + v \frac{\partial u}{\partial y} - fv &= F_x + \frac{\tau_{wind_x} - \tau_{bottom_x}}{\rho H} - \left(\frac{1}{\rho} \frac{\partial Pa}{\partial x} + g \frac{\partial \zeta}{\partial x} \right) - \frac{\partial V_M}{\partial x} \\ \frac{\partial v}{\partial t} + u \frac{\partial v}{\partial x} + v \frac{\partial v}{\partial y} + \underbrace{fu}_{\text{Coriolis}} &= F_y + \frac{\tau_{wind_y} - \tau_{bottom_y}}{\rho H} - \left(\frac{1}{\rho} \frac{\partial Pa}{\partial y} + g \frac{\partial \zeta}{\partial y} \right) - \frac{\partial V_M}{\partial y} \end{aligned} \quad (2)$$

time
advection
friction stress
pressure
tidal potential

Continuity Equation:

$$\frac{\partial \zeta}{\partial t} + \frac{\partial(Hu)}{\partial x} + \frac{\partial(Hv)}{\partial y} = 0 \quad (3)$$

With:

- u the zonal and v the meridional components of barotropic currents,
- ζ the sea surface elevation and H the total height of the water column.

A first difference between the different 2D models is the physical parameterisation of the different terms involved in these equations:

- the possibility to take into account a constant or variable Coriolis force f ,
- the possibility to take into account the tidal potential V_M ,
- the possibility to take into account atmospheric (Pa, wind) forcing and the way wind stress τ_{wind} is modelled,
- the way to model bottom friction τ_{bottom} ,
- the way to model inner frictions forces (F_x, F_y) due to viscosity and mainly to turbulence.

Other sources and sinks can be taken into consideration in the hydrodynamic equations. For example:

- the effect of waves on the currents
- river discharges

As 3D models, some 2D models (TELEMAC 2D for example) give the possibility to use a 2 dimensional system without assuming hydrostatics hypothesis. This is the Boussinesq formulation, an extension of the Saint Venant equations taking partly into account the vertical velocity.

2.2.2 Numerical resolution and Computational Grids

Another major difference between the hydrodynamic models is the computational mesh and the numerical schemes used to solve the Partial Differential Equations system (2D or 3D).

Three mathematical properties characterise the quality of a numerical scheme:

- the accuracy of the scheme : when the integration steps (temporal and spatial) tend toward zero the numerical scheme should tend to the continuous differential equation.
- the convergence of the scheme: the numerical solution should tend toward the exact solution when the integration steps (temporal and spatial) tend toward zero.
- the stability of the scheme: the solution should not diverge.

Another important point is the monotony and the order of the scheme. The implemented scheme should be a compromise between accuracy with risk of oscillation and guaranty of monotony but too much diffusivity. Finally, a numerical scheme should be conservative (mass, motion, heat conservation).

Most often used resolution methods are:

- finite differences methods
- finite volumes methods
- finite elements methods
- spectral methods

The main advantage of finite elements methods and finite volumes methods is that they can be used on unstructured meshes which facilitate the numerical modelling for complex geometries of coastal regions.

2.3 TIDAL MODELS

2.3.1 TELEMAC-2D

2.3.1.1 Computational Grid

TELEMAC-2D solves the Saint-Venant equations using the finite-element or finite-volume method. Finite element method is the default and the most often used. Equations are solved in two stages. Convection terms are solved first, followed by propagation and diffusion terms. Telemac offers different numerical schemes to solve the convection terms, the characteristics method is the default one. Propagation and convection are solved using the finite element method (various solvers for the linear system).

The finite element computation mesh of triangular elements enables to adapt the horizontal step at the study area: large mesh grid near the border, refined mesh grid at the coast and particularly near the areas of interest (see Figure 2). One should choose the spatial resolution of the computational grid such that relevant spatial details in the bathymetry are properly resolved. The grid can be either in spherical coordinates (for large domains) or projected (in meters, for small domains like coastal regions or harbors).

In the nearshore region, Telemac takes into account wet and dry cells.

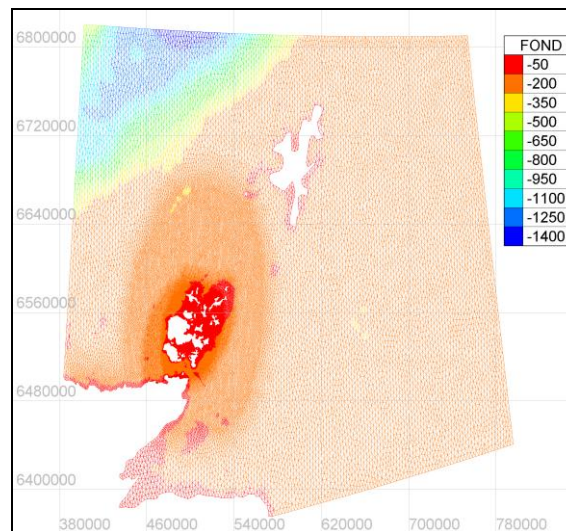


Figure 2 Example of mesh grid

2.3.1.2 Modelled Processes

- The Coriolis force is taken into account by default but can be deactivated by the user. If the model grid is in spherical coordinates, the Coriolis coefficient ($f = 2 \omega \sin(\text{lat})$, with $\omega = 7.292 \times 10^{-5}$ rd/s) is variable and calculated by the software. Otherwise, the coefficient is a constant (which is satisfying enough for small domains) and should be prescribed by the user.
- Tidal potential can be taken into account.
- Wind stress at the surface depends on the 10m high wind $\vec{W}_{10} \begin{pmatrix} U_{10} \\ V_{10} \end{pmatrix}$

$$\begin{cases} F_{wind_x} = \frac{\tau_{wind_x}}{\rho H} = \frac{1}{H} \frac{\rho_a}{\rho} a_{wind} U_{10} \|\vec{W}_{10}\| \\ F_{wind_y} = \frac{\tau_{wind_y}}{\rho H} = \frac{1}{H} \frac{\rho_a}{\rho} a_{wind} V_{10} \|\vec{W}_{10}\| \end{cases} \quad (7)$$

$\frac{\rho_a}{\rho} a_{wind}$ being a constant coefficient given by the user.

- Bottom Friction dependency with barotropic velocity can be modeled using different laws:

- No friction
- Haaland Law
- Chezy Law
- Strikler Law
- Manning Law
- Nikurades Law

Bottom friction can be expressed as

$$\begin{cases} F_{bottom_x} = \frac{\tau_{bottom_x}}{\rho H} = \frac{g}{C^2 H} u \|\vec{u}\| \\ F_{bottom_y} = \frac{\tau_{bottom_y}}{\rho H} = \frac{g}{C^2 H} v \|\vec{u}\| \end{cases} \quad (8)$$

Where the Chézy law is applied C is constant.

When $C = KH^{1/6}$, K is a Strickler coefficient

When $C = \frac{H^{1/6}}{m}$, $m=1/K$ is a Manning coefficient

Strikler, Chézy or Manning coefficient are given by the user. They can be a constant (default) or they can be variable in space or time (user defined).

- The effect of turbulence can be represented by four different ways:
 - Similarly to molecular viscosity by defining a global viscosity coefficient.
 - With an Elder model
 - With a $k-\varepsilon$ model
 - With a Smagorinsky model

2.3.1.3 Input Data

- At the open boundaries sea surface elevation and currents (or flows) must be specified. If only sea levels are available, the Thomson method will use the characteristics method to appraise the value of currents along the boundaries.
- Telemac-2D takes into account wind and pressure influence. The integration of a meteorological forcing variable in time and space is possible but has to be done by the user.
- Telemac can compute wave induced currents by coupling with a sea state model (preferably TOMAWAC, the spectral wave model developed in the Telemac system).

3 MODEL INTERCOMPARISON AT ORKNEY, UK

3.1 SITE SUMMARY

3.1.1 Location

The test site chosen for the hydrodynamic modelling study is located in the Orkney Islands, near Eday Island. In this site, in-situ measurements of currents and sea levels are available. They were kindly provided by EMEC.

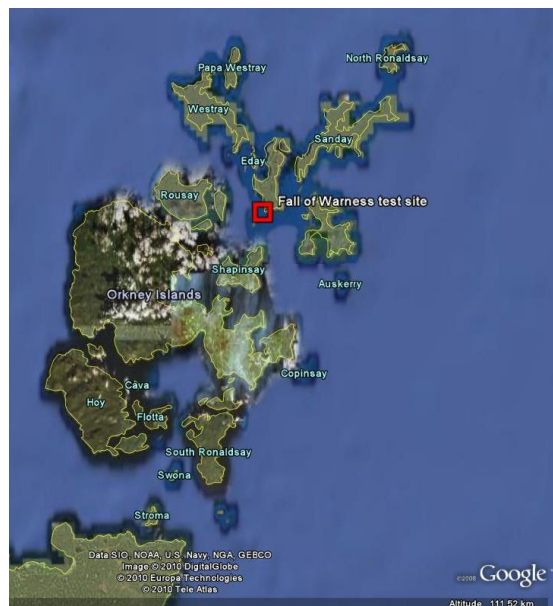


Figure 3 Location of the area of interest

3.1.2 Bathymetry

The model grid has been computed using a 500m resolution bathymetry of the Orkney island (source: EMEC) given on Figure 4. In addition, 1' grid GEBCO¹ bathymetry has been used where the finest bathymetry is not available (see Figure 5).

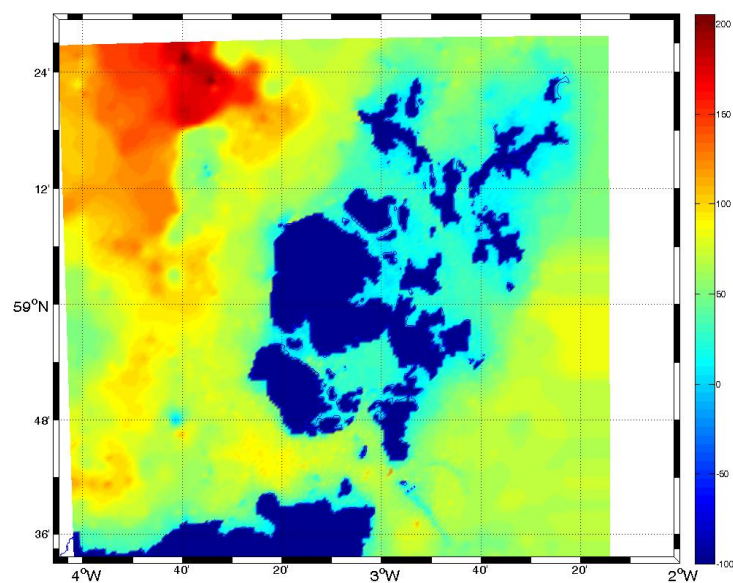


Figure 4 500m fine bathymetry (source EMEC)

¹ General Bathymetric Chart of the Oceans (GEBCO). <http://www.gebco.net/>

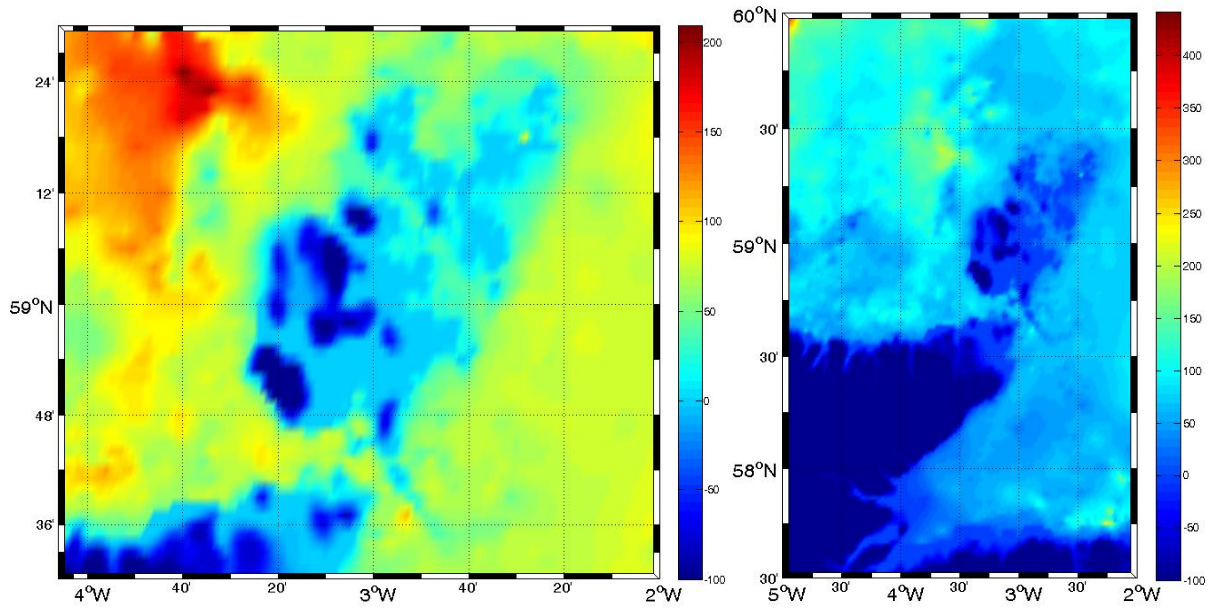


Figure 5 GEBCO bathymetry

3.2 CALIBRATION AND VALIDATION DATA

3.2.1 Presentation of hydrodynamic validation data

Current profiles and water depth measurements have been realised in the area of interest at the locations given on Figure 6.

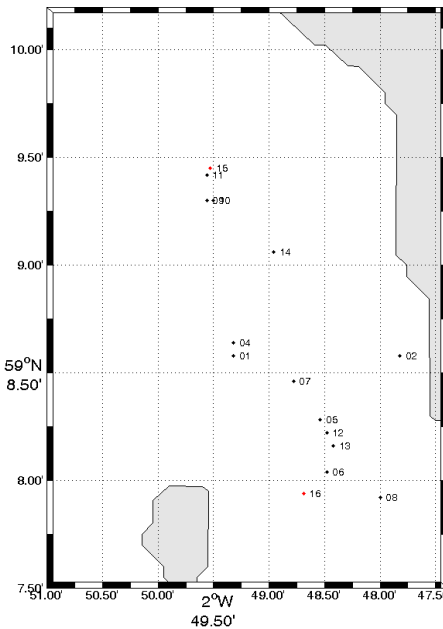


Figure 6 Location of currents measurement points

During the test simulation period, measurements are available at points 6 and 7. At point 7, located in 52.6m depth, data is available every 10 minutes. At point 6, located in 41.8m depth, it is available every 20s but only 10 minutes values have been used. Figure 7 shows, for example, current profiles measured at point 7.

To do the comparison with model results, depth averaged velocity was estimated using 60% height current (as advised in ²).

² Eloi Droniou, “Processing and quality control of currents and waves for FoW-SMADCP-7”, The European Marine Energy Centre Ltd, 2008

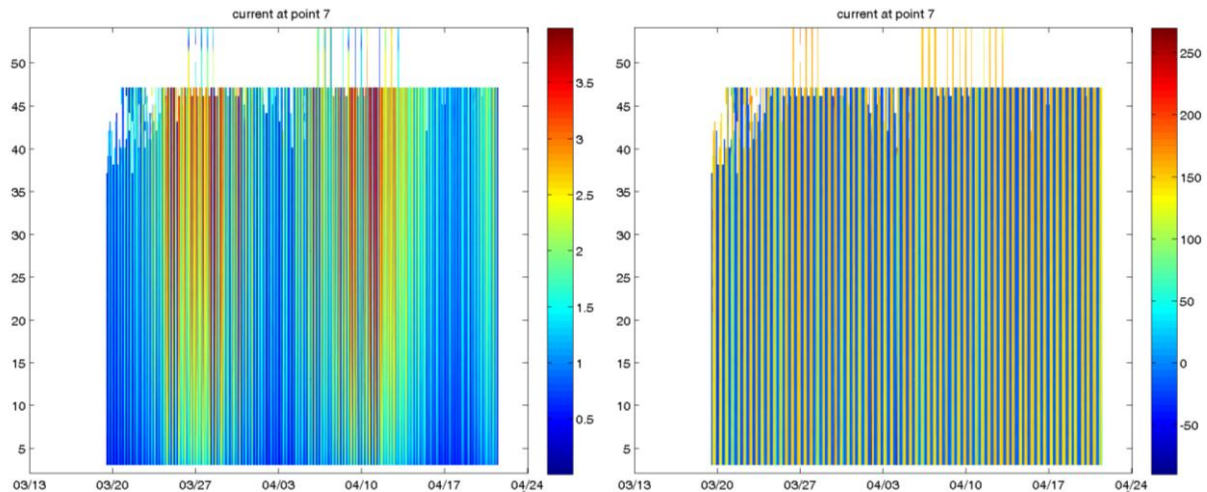


Figure 7 Current speed and direction evolution at point 7

Moreover, results from the model can also be compared with sea level in the following harbours (see Figure 8):

- Wick
- Lerwick
- Aberdeen

In these harbours, tidal level can be derived from the French Marine Oceanographic and Hydrodynamic Service SHOM³ harmonic predictions in harbours. Tide gauge measurements are also supplied by the British Oceanographic Data Centre as part of the function of the National Tidal & Sea Level Facility⁴.

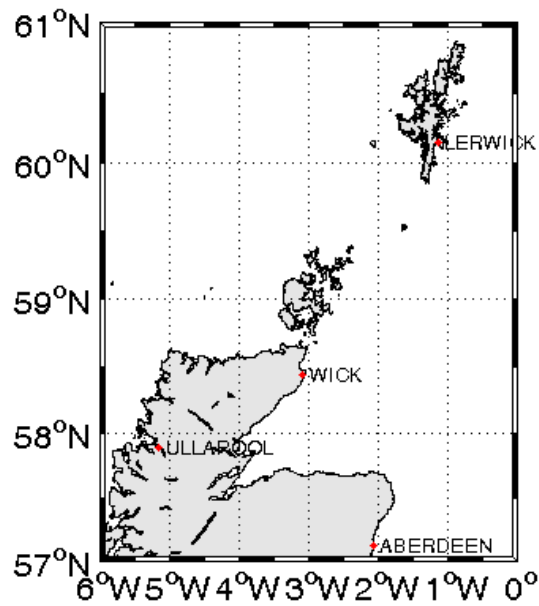


Figure 8 Location of harbour

3.2.2 Presentation of meteorological forcing data

Times series of wind speed and direction (10m above the ground) and of pressure (at MSL) at 59°N - 3°W have been extracted from the « Global Forecast System »⁵ model results. GFS is a global 1° meteorological model from the « National Center for Environmental Prediction ». 3-hours time series are available from 2000 to 2008. They have been used to derive wind statistics.

³ SHOM harmonic tidal prediction in harbours

http://www.shom.fr/ann_marees/cgi-bin/predit_ext/choixp?opt=&zone=9&port=0&portsel=map

⁴ UK National Tidal and Sea Level Facility <http://www.pol.ac.uk/ntslf/>

⁵ GFS <http://www.nco.ncep.noaa.gov/pmb/nwprod/analysis/>

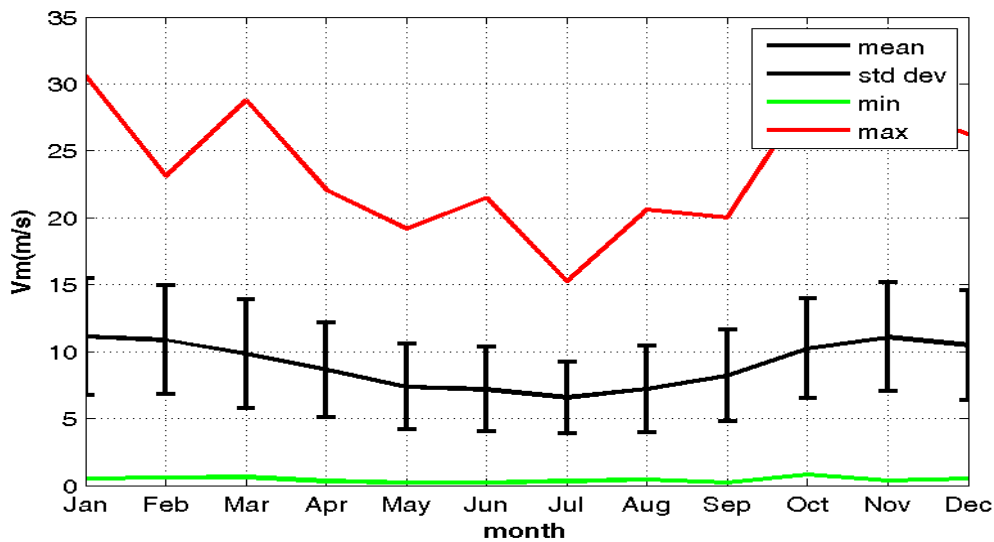


Figure 9 Monthly wind speed statistics at point 59°N-3°W

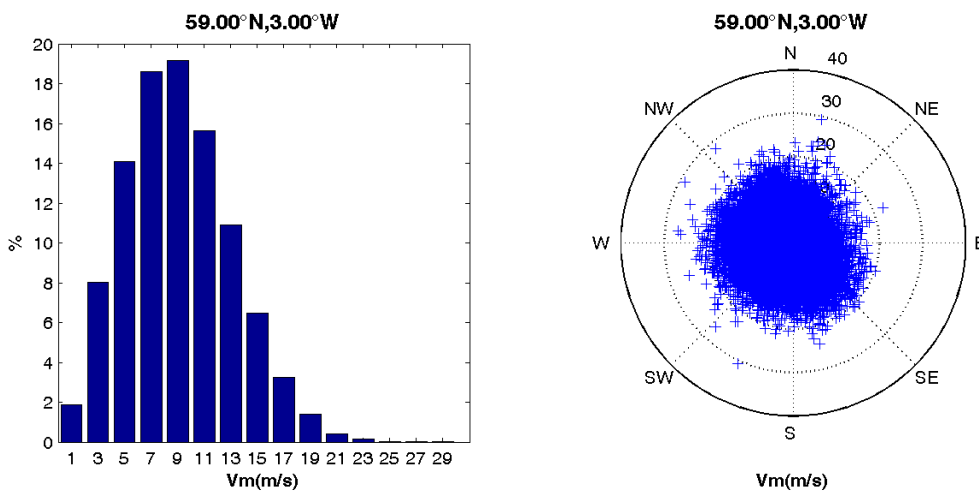


Figure 10 Wind Speed distribution (left) and Wind Speed/Direction scatter plot (right) at point 59°N-3°W

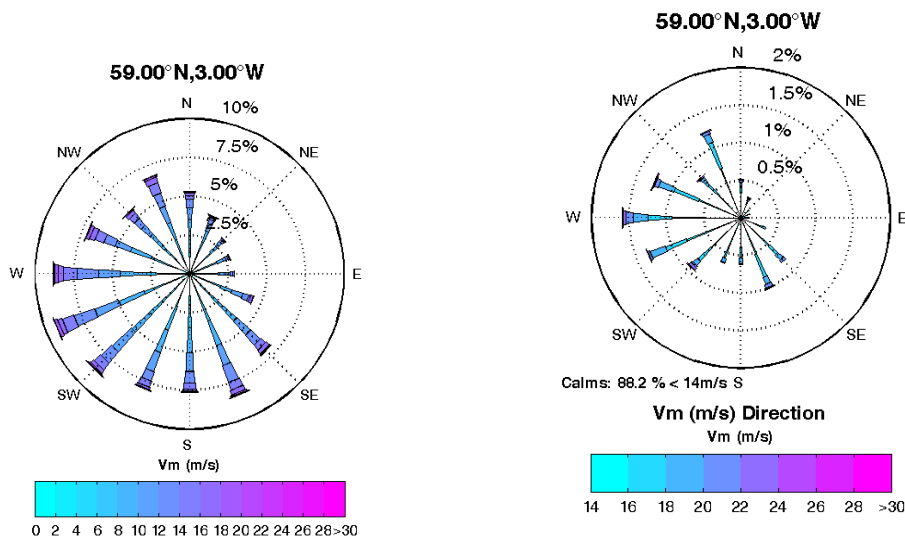


Figure 11 Wind Speed/Direction roses for total wind (left) and strongest winds (right) at point 59°N-3°W

Figure 9 shows that wind speed monthly mean ranges from 7m/s from June to August to 11m/s from November to February. Maximum wind speed can be over 25m/s (in January, March, October November and December) and reach 30m/s (during the January 2005 storm). But such events are very scarce. 88.2% of winds are lower than 14m/s. Figure 11 points out that wind blows mainly from SE to NW and that the strongest winds come mainly from West.

3.3 TELEMAC-2D MODELLING

3.3.1 Model Setup

To predict tidal current and level in the Fall of Warness test site, a telemac-2D model has to been implemented (see Figure 12).

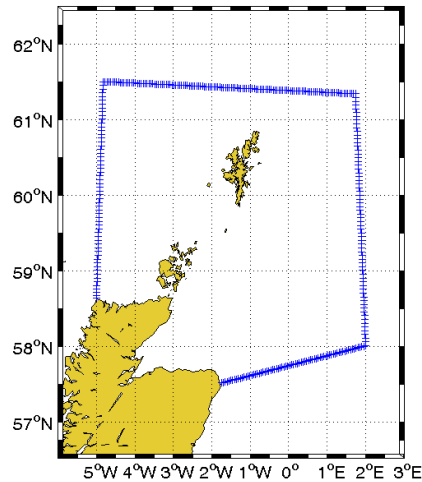


Figure 12 Hydrodynamic model domain

TELEMAC-2D solves the two dimensional Saint-Venant equations using the finite-element method on the computational mesh grid given on Figure 13. It is made up of 46890 nodes and 90970 triangular elements. The size of the mesh goes from 0.05° at the open boundaries to 0.005° near the site of interest. X and Y coordinates are in meters UTM.

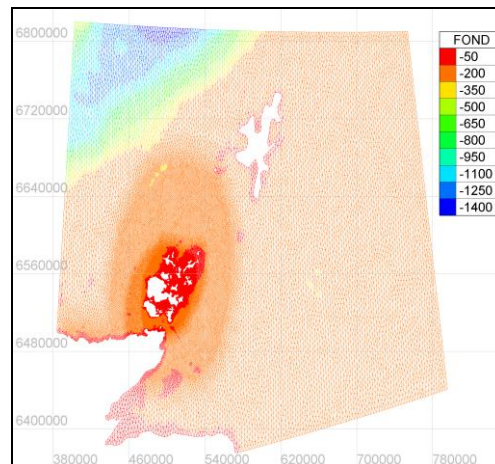


Figure 13 Model mesh grid

At its open boundaries the model can be forced by water level or/and currents. Only water level tidal conditions are provided here. They are computed using FES2004⁶ harmonic components database.

No meteorological forcing is taken into account in the reference simulation. However, the influence of wind and pressure forcing will be studied later using GFS data.

Water level and velocity results are computed taking into account:

- Coriolis force (assuming to be a constant)
- Bottom friction modelled by a Chezy law
- Turbulence viscosity computed with the Smagorinsky model.

The reference simulation has been run with a Chezy law coefficient of 60.

The drying cells ability of the Telemac2D model has not been used in the simulation. A minimum water depth of 2.5m has been imposed in the model so that all the cells are always wet.

⁶ FES2004 tidal atlas. www.legos.obs-mip.fr/fr/soa/produits/modele-fes/

3.3.2 Model Output

A test simulation has been run from 01 to 20 April 2005 without atmospheric forcing. Figure 14 to Figure 16 give example of current maps in the Orkney Islands and in the area of interest, near Eday Island during flood and ebb maximum (around High Tide ± 3 hours). They show that tidal currents in the area of interest are important. Unfortunately, the available bathymetry and consequently the model grid are not fine enough to reproduce entirely the complexity of the currents in the study area.

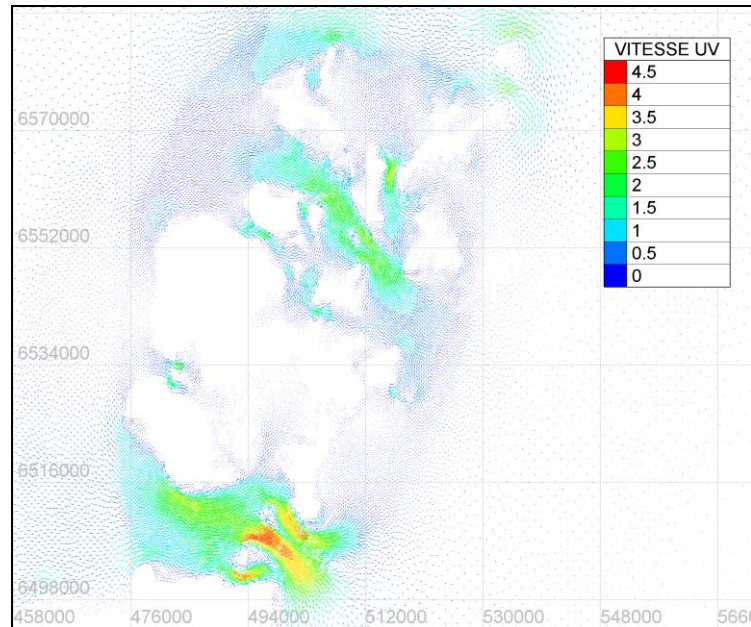


Figure 14 Current map in the Orkney Islands on 07/04/2005 at HT+3h

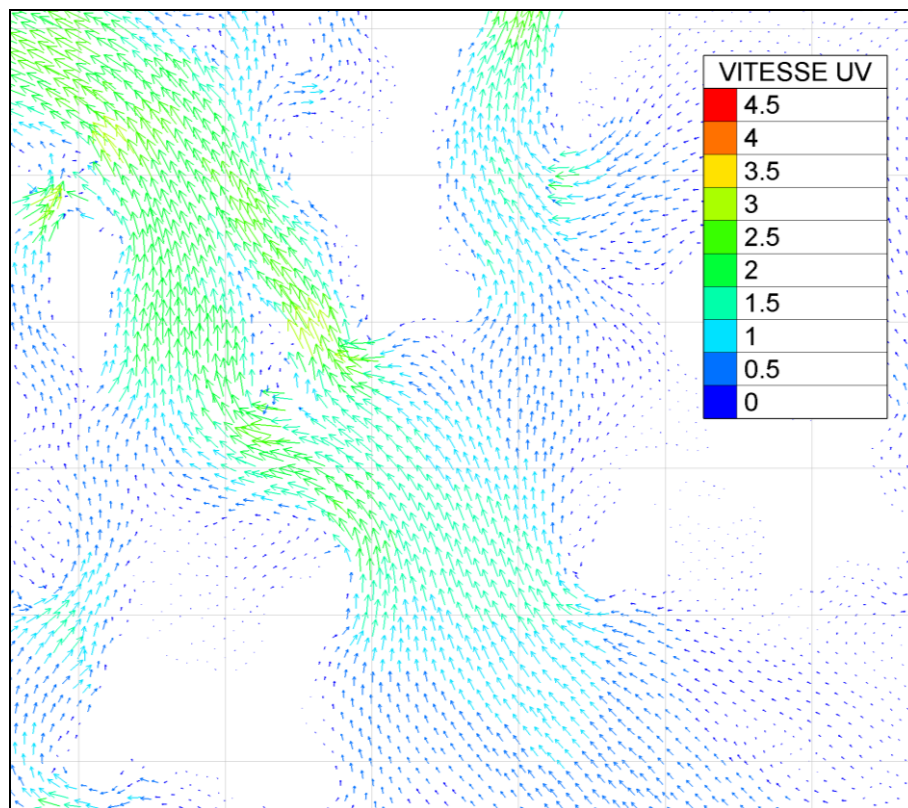


Figure 15 Current map at Fall of Warness on 07/04/2005 at ebb HT+3h

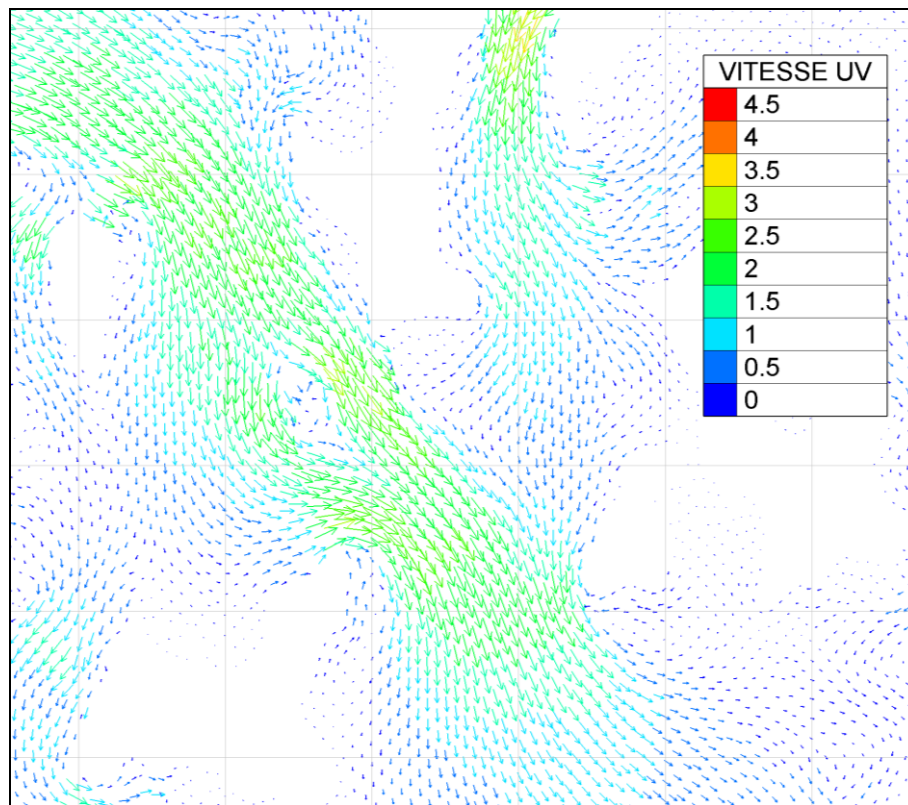


Figure 16 Current map at Fall of Warness on 07/04/2005 at flood HT-3h

Tidal elevations of sea level and currents from model results have been compared with available data.

- *Sea levels*

Using SHOM³ database, sea levels at Wick, Lerwick and Aberdeen have been predicted during the simulation period. Figure 17 gives predicted and modelled tidal elevation (relatively to MSL) 30-minutes time series at these three harbours. It points out that model results are in good accordance with astronomic tidal level. At Lerwick and Wick model results are in phase with prediction and tidal amplitude seems somehow overestimated. However, Figure 18 shows that sea levels are rather similar. At Aberdeen model results are slightly out of phase. That is why the corresponding scatter plot is not given. Aberdeen is very close to the model boundary, it can explain the phase shift.

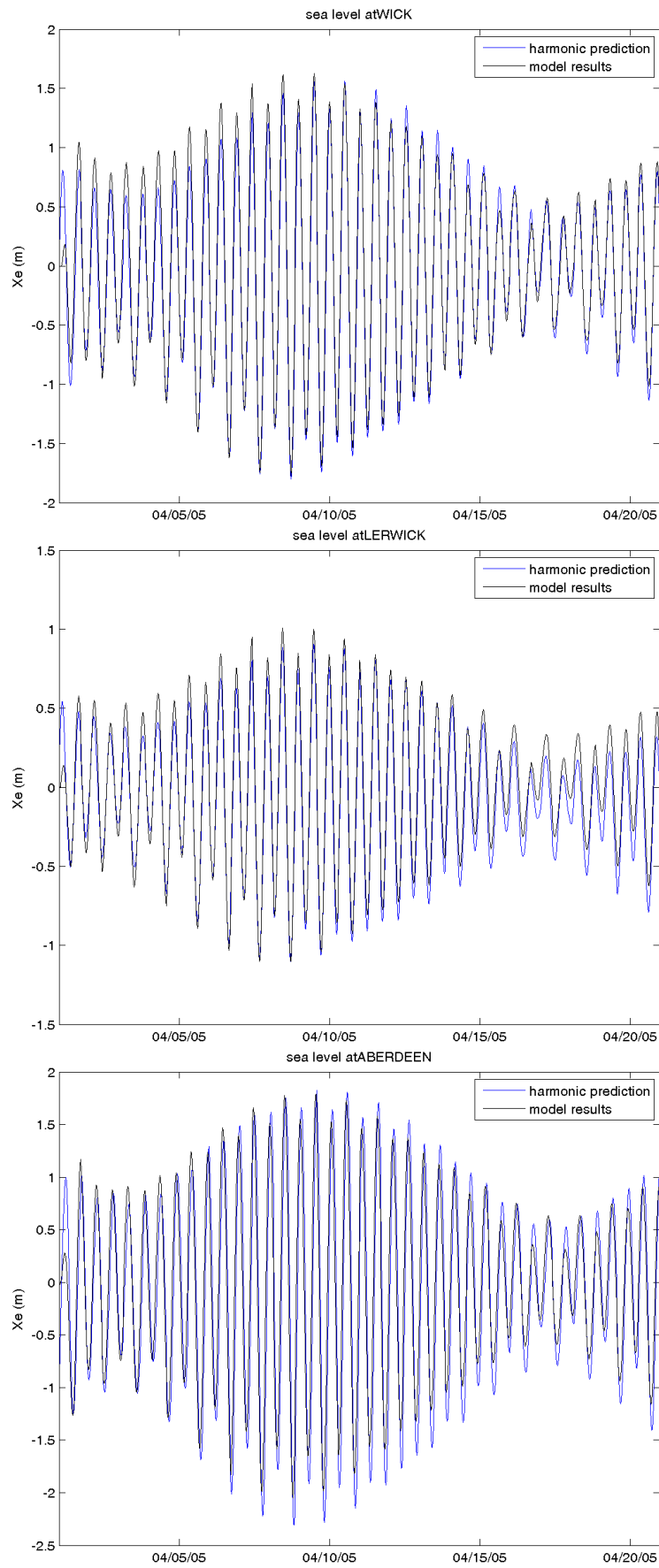


Figure 17 Tidal sea level comparison in harbours

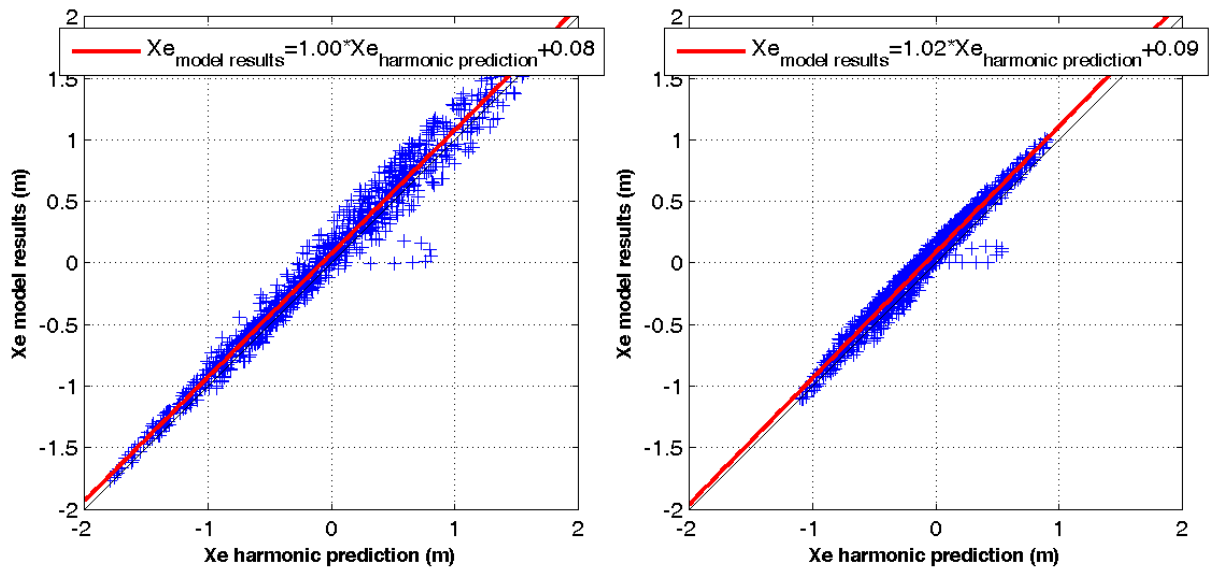


Figure 18 Predicted against modelled sea level at Wick (left) and Lerwick (right)

As visible on Figure 19 sea level evolution at point 7 is also relatively well represented by the model. Observed differences on amplitude can come from model error due to imprecision in depth in the area (only 500m bathymetry) for example or meteorological effect on measured level.

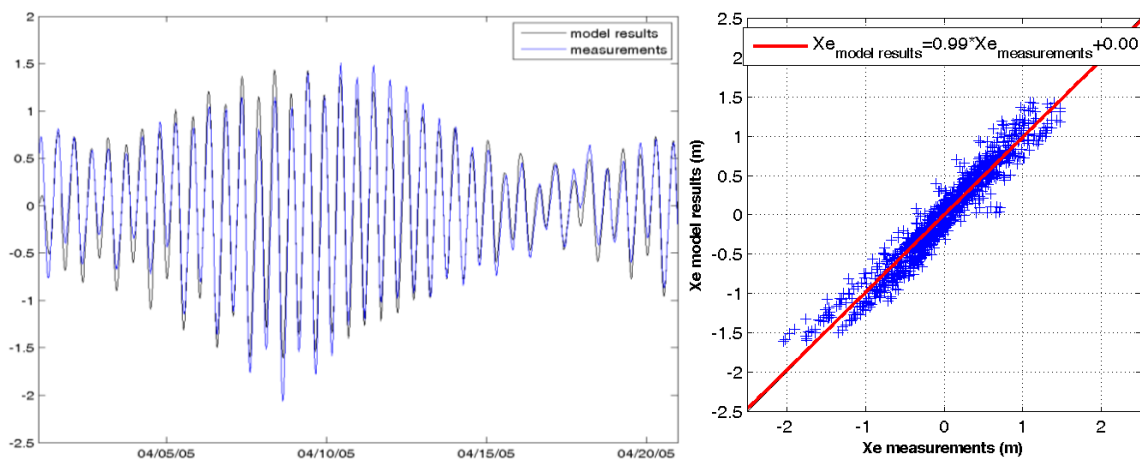


Figure 19 Modelled against measured sea level at point 7

- *Currents*

Currents measured at point 7 flow alternatively toward S-SE and N-NW. This oscillation is well reproduced by the model (see Figure 21, Figure 22) and current intensity is rather satisfying. However the scatter plot on Figure 20 points out that the model tends to underestimate the highest values of current. This underestimation is probably linked with bathymetry approximation. However, giving the test area and the available bathymetry, results are rather satisfying.

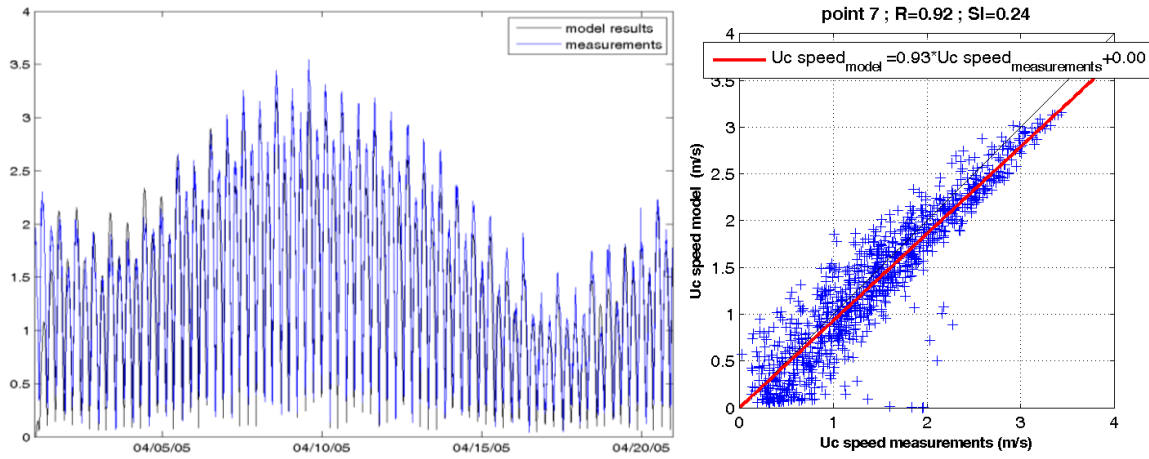


Figure 20 Modelled against measured current intensity at point 7

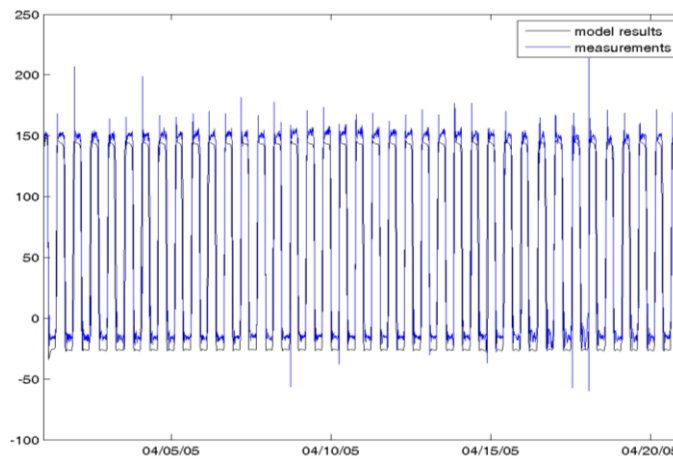


Figure 21 Modelled against measured current direction at point 7

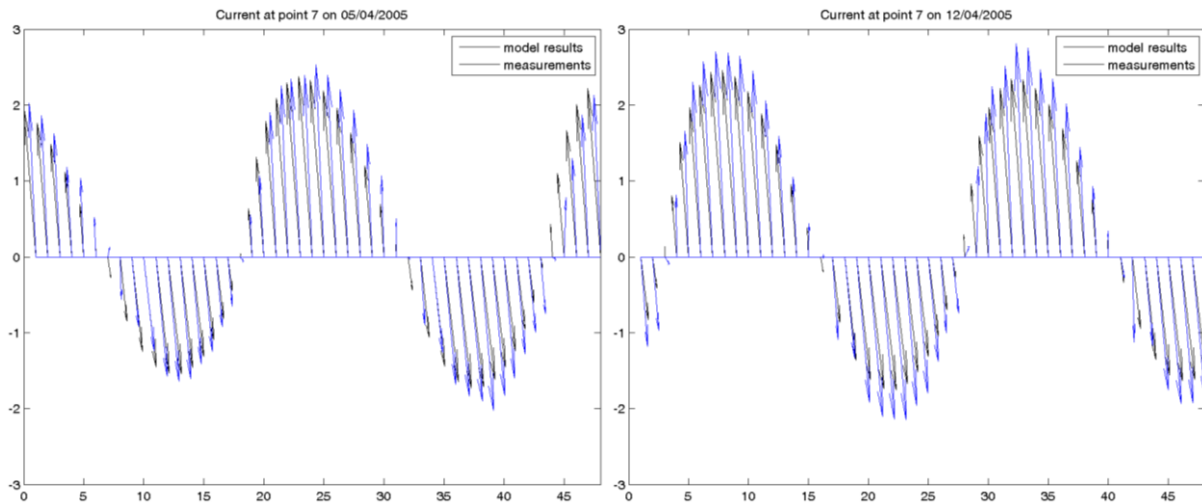


Figure 22 Modelled and measured current on 05/04/2005 (left) and 12/04/2005 (right) at point 7

At point 6, model results are rather similar to point 7 results. The underestimation is slightly more significant.

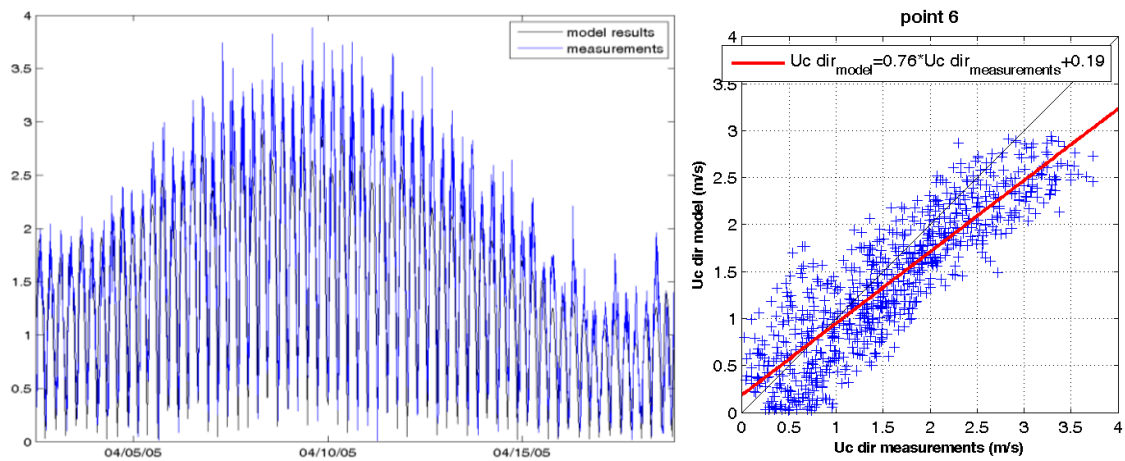


Figure 23 Modelled against measured current intensity at point 6

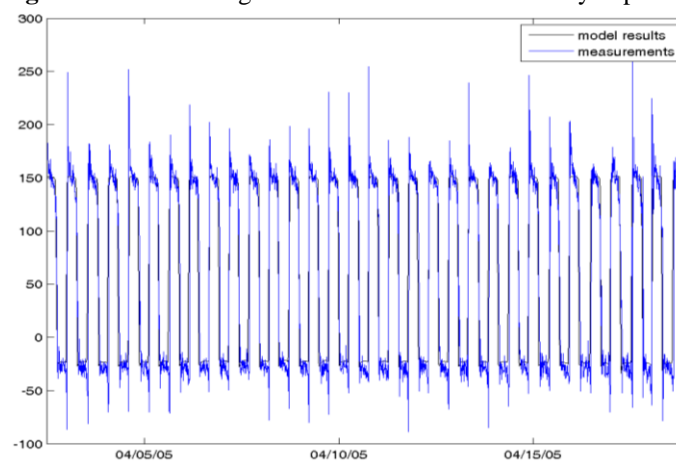


Figure 24 Modelled against measured current direction at point 6

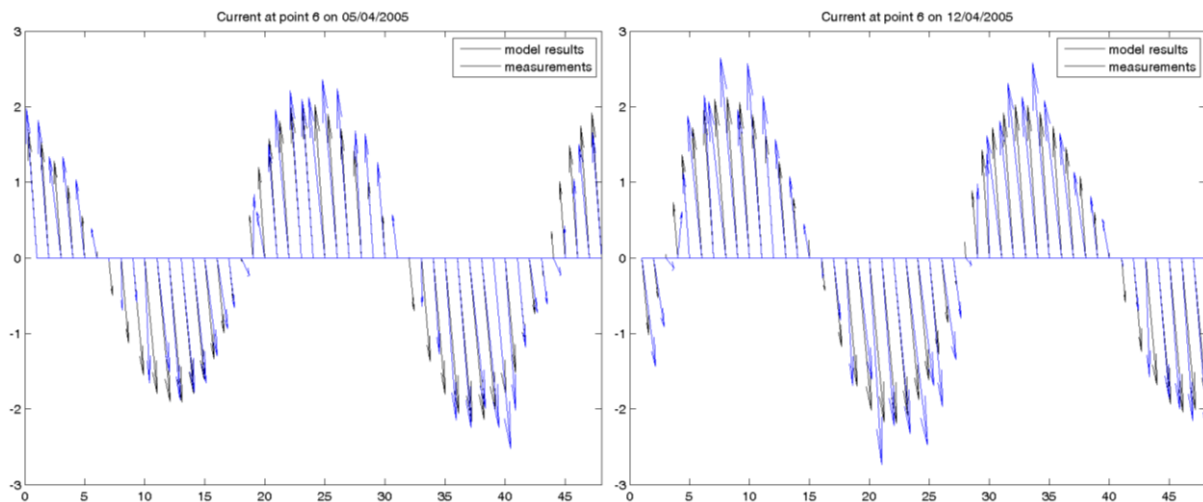


Figure 25 Modelled and measured current on 05/04/2005 (left) and 12/04/2005 (right) at point 6

3.3.3 Adjustment of bottom friction coefficient

Error on modelled currents probably comes from the bathymetry accuracy. Indeed, given the area of interest, the model implementation requires a fine representation of the bathymetry. This error can be reduced by modifying the bottom friction coefficient. The bottom friction coefficient can be either homogeneous on the entire model or it can be defined on different areas. Here, as current measurements are only available in a very specific area of the model, the coefficient is homogeneous and is adjusted to better fit the local measurements at one selected point.

- Influence of bottom friction coefficient

Figure 26 and Figure 27 point out the influence of friction coefficient for Chezy coefficient of 30 and 80. On Figure 26, model results for the two friction coefficients are compared with measurements at point 7. Figure 27 gives simultaneous (06/04/2005 at 13h) examples of currents maps in the area of interest. They show that with a smaller Chezy coefficient, bottom friction is higher and then currents are lower.

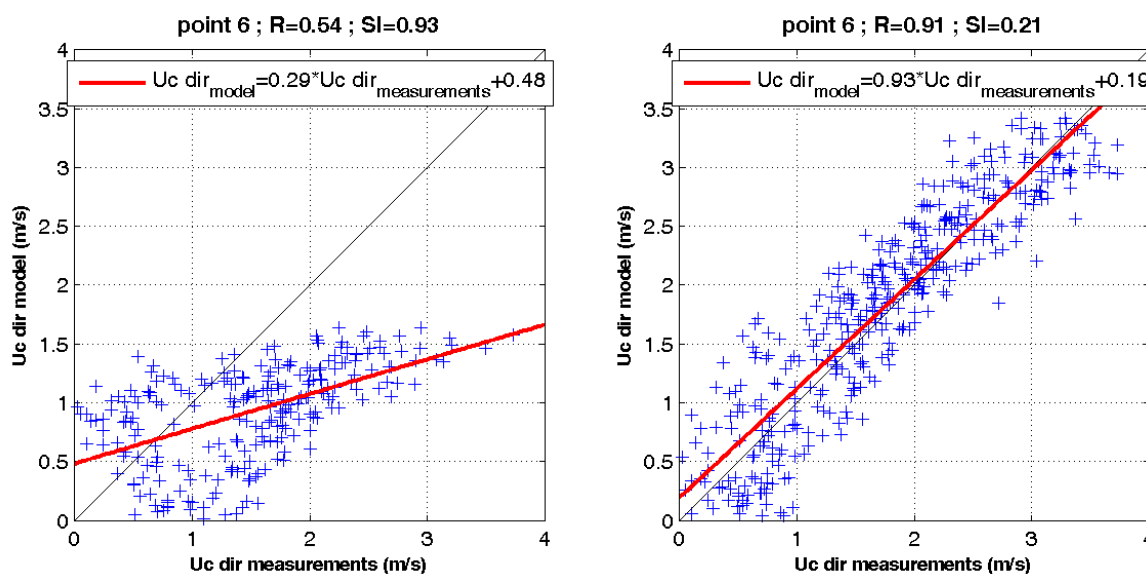


Figure 26 Modelled against measured current intensity at point 6 for Chezy coefficient of 30 (left) and 80 (right)

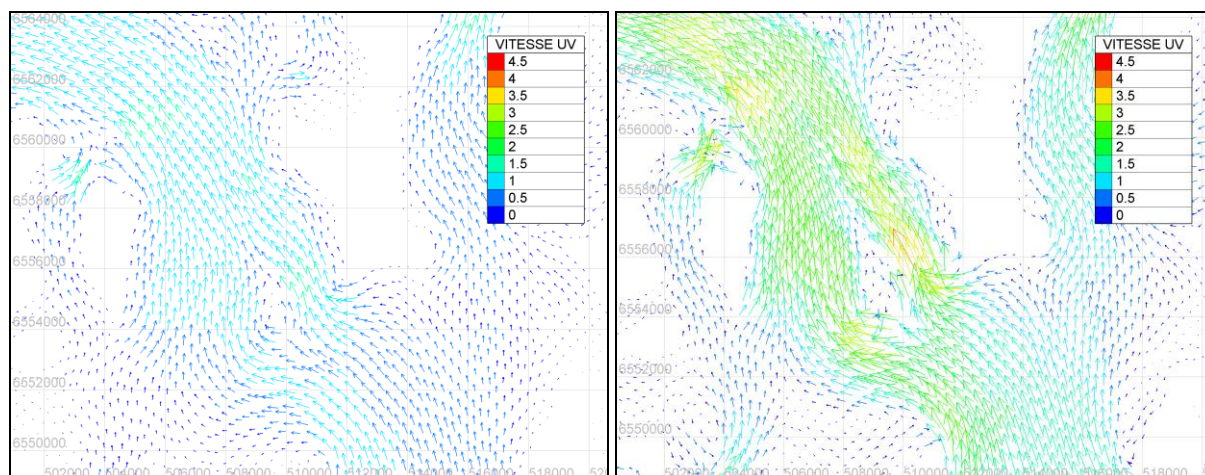


Figure 27 Example of current map from model results with Chezy coefficient of 30 (left) and 80 (right) on 06/04/2005 at 13h

- *Adjustment of bottom friction coefficient*

Model results have been compared with measurements at point 6 and 7 for different Chezy coefficients (60, 70 and 80). As visible on Figure 28 and Figure 29 a coefficient of 70 leads to more satisfying results at point 7.

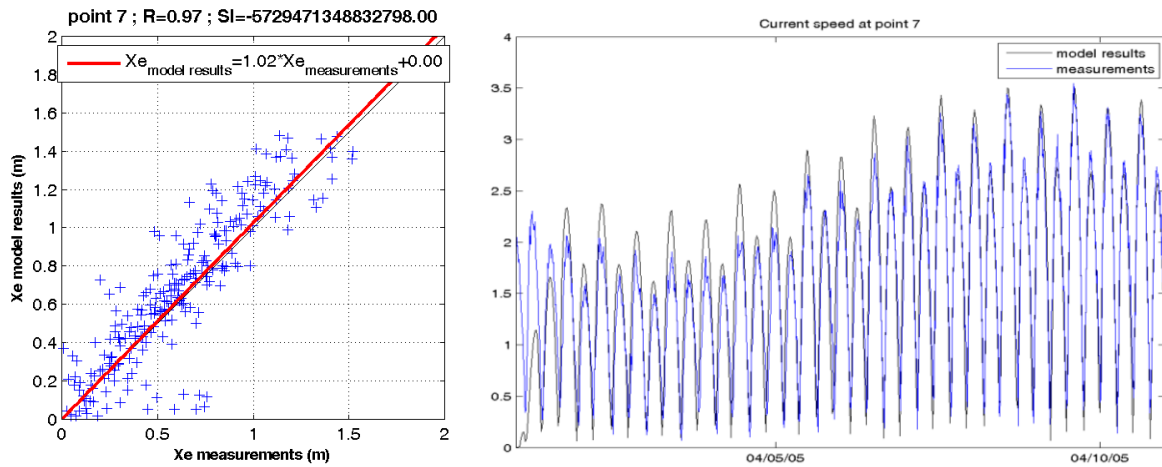


Figure 28 Modelled against measured current intensity at point 7

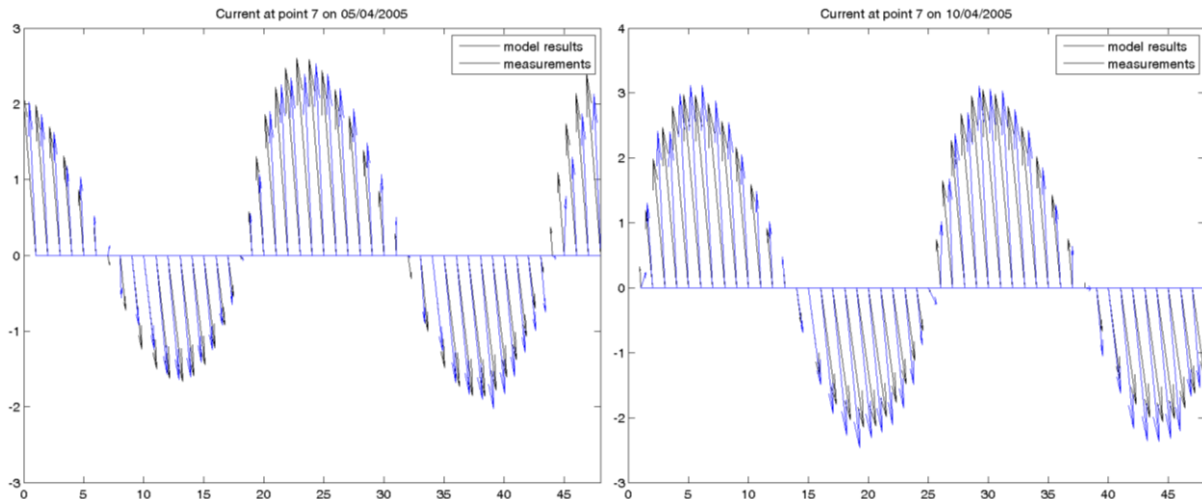


Figure 29 Modelled and measured current on 05/04/2005 (left) and 10/04/2005 (right) at point 7

3.3.4 Influence of meteorological forcing

Storm surge is the difference between observed sea level and predicted tidal sea level. This residual is generated by specific weather conditions (winds and pressure). Surge has first been derived from measurements then from model results.

- *Meteorological conditions during the selected measurement period*

Figure 30 gives wind and pressure evolution during the test simulation period. Wind intensity is around 10m/s during a great part of the simulation with a peak to 20m/s from North (350°) on 07 April 2005. Pressure is relatively stable around 1 atmosphere. The grower low-pressure event observed is 30mbar on 07 April 2005 again.

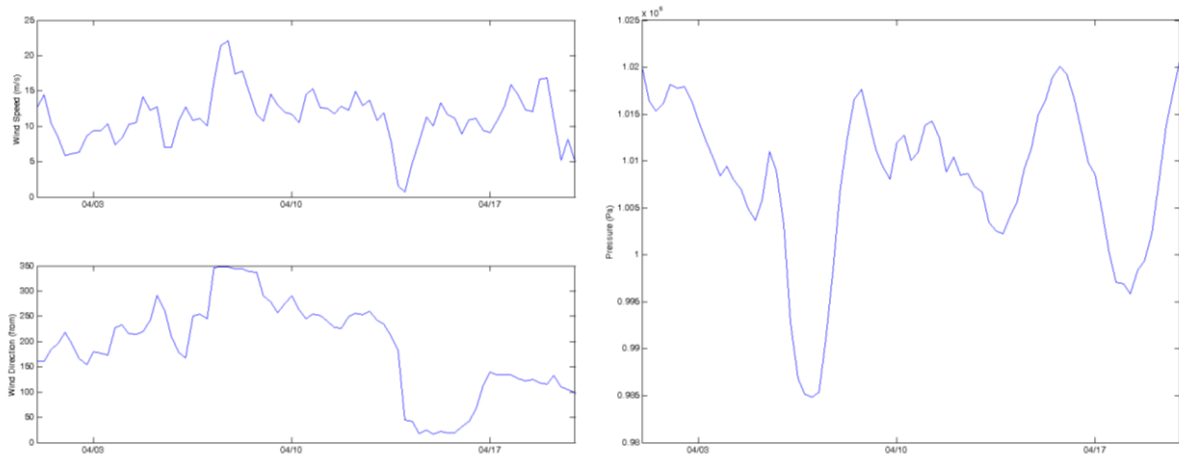


Figure 30 Wind and pressure time series at 59°N - 3°W from 01 to 20 April 2005

- *Surge measured at Wick harbour*

The Oceanographic Data Centre⁴ provides sea level as well as residual measurements from the UK tide gauge network. Quality checked time series at Wick for year 2005 are given on Figure 31.

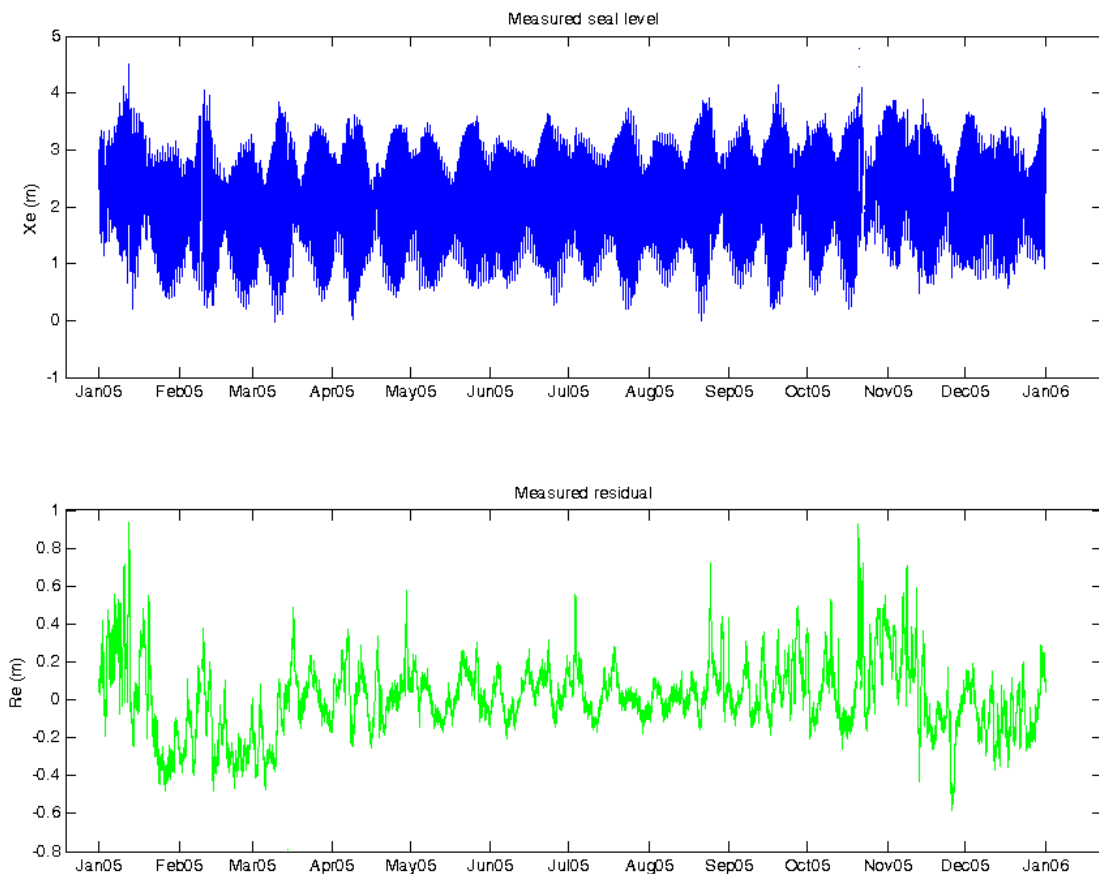


Figure 31 Sea level and residual at Wick

Figure 31 example emphasizes that meteorological residual is mainly lower than 20cm. However, during some particular events, residual can reach 80cm. Given the sea level time series, the peak observed at the mid of October is probably due to measurements hurdles. On the contrary, it seems that the higher values observed in January 2005 are realistic as they occurred during an important storm event.

The inverted barometer approximation is frequently used to estimate surge without numerical modelling. Given the following relation:

$$\Delta X_e = \frac{1}{\rho g} (P_{ref} - P)$$

It assumes that a 1mbar low pressure leads to a 1cm surge.

Figure 32 shows that this approximation satisfyingly represents the global residual evolution at Wick harbour. However some events and particularly the strongest ones are underestimated. Indeed, the inverted barometer approximation neglects the dynamic effects of pressure as well as the effects of winds.

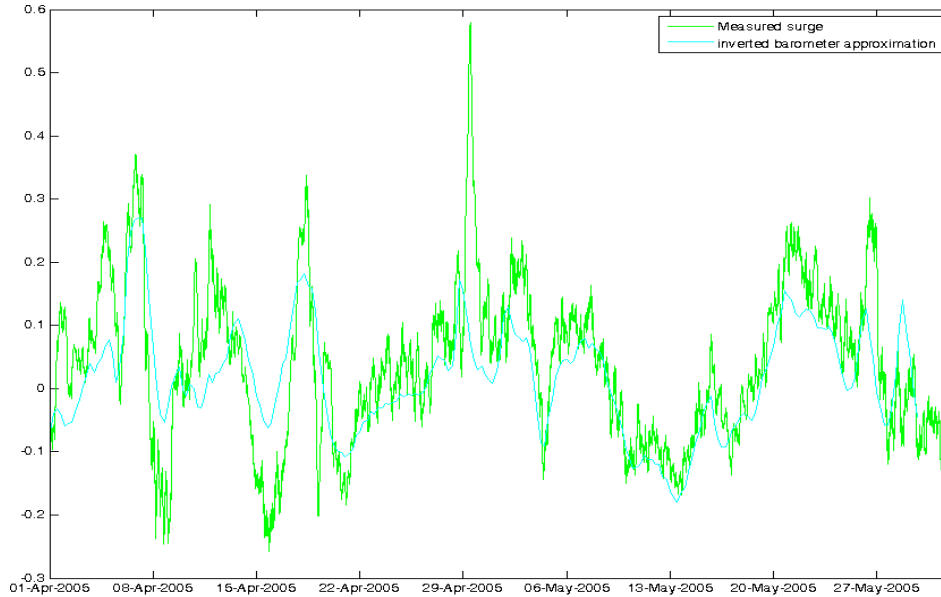


Figure 32 Measured residual level and inverted barometer approximation at Wick

- *Surge measured at Fall of Warness*

As the tidal level is not known for the measurement points in Fall of Warness, storm surge has been evaluating using the linear filter “Demerliac”⁷. Demerliac filter is a low pass filter removing short wave lengths with period lower than 25h. It thus removes most of tidal components. Results from the measurements have also been compared with the inverted barometer approximation results on Figure 33. It emphasizes the influence of winds. Particularly on the 07/04/2005, while low pressure is predicted, it seems that the strong wind blowing from North generates a negative residual of around 30cm.

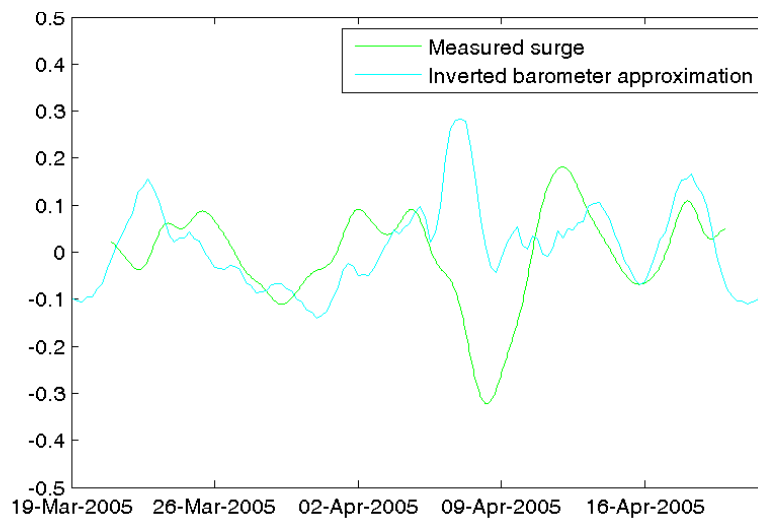


Figure 33 Measured residual level and inverted barometer approximation at point 7

⁷ M.A. Demerliac, « Le niveau moyen de la mer, calcul du niveau moyen journalier »

- *Estimation of the Surge with the model*

Estimation of the surge from the available measurements emphasized that:

- surge can be significant in the area
- the inverted barometer approximation is not satisfying enough

That is why a hydrodynamic model should be used to predict surge. The model domain is not large enough to reproduce wind induced surge due to the propagation in shallow water on the shelf. So as to satisfyingly reproduce surge in the model, it is no longer possible to force open boundaries with tidal sea level only. That is why, to study the estimation of surge by the model, sea level condition at its open boundaries are no longer derived from harmonic composition with FES 2004 but they are evaluated using a larger model.

This larger model is forced by:

- FES2004 sea level prediction at the open boundaries
- Wind and pressure atmospheric condition at the surface.

Figure 34 gives preliminary results obtained using this model to produce local model open boundaries condition. The origin of the time gap observed between model results and measurements has to be investigated.

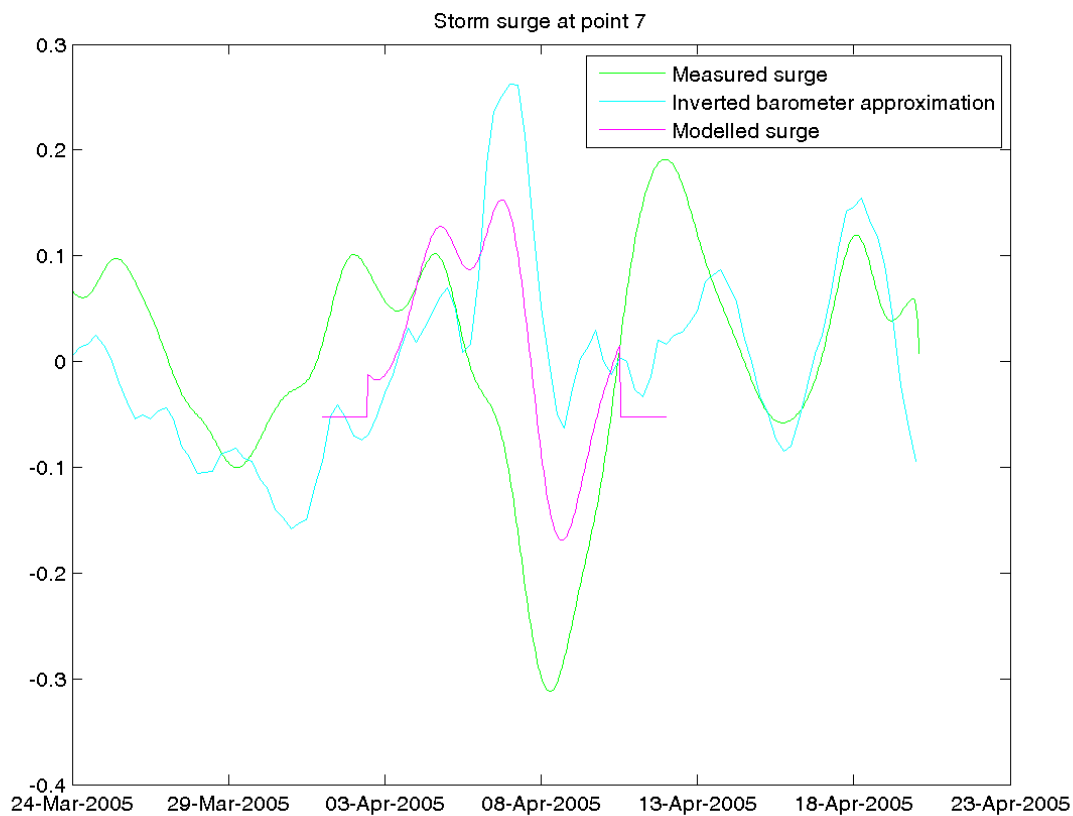


Figure 34 Measured and modelled Storm surge at point 7

3.4 MIKE21 MODELLING

3.4.1 Model Setup

With the available computer resources, a model was set up of a smaller area of the Orkney Islands, using Mike21. The same bathymetry dataset was used. The sub-mesh consisted of 37688 nodes and 72806 elements.

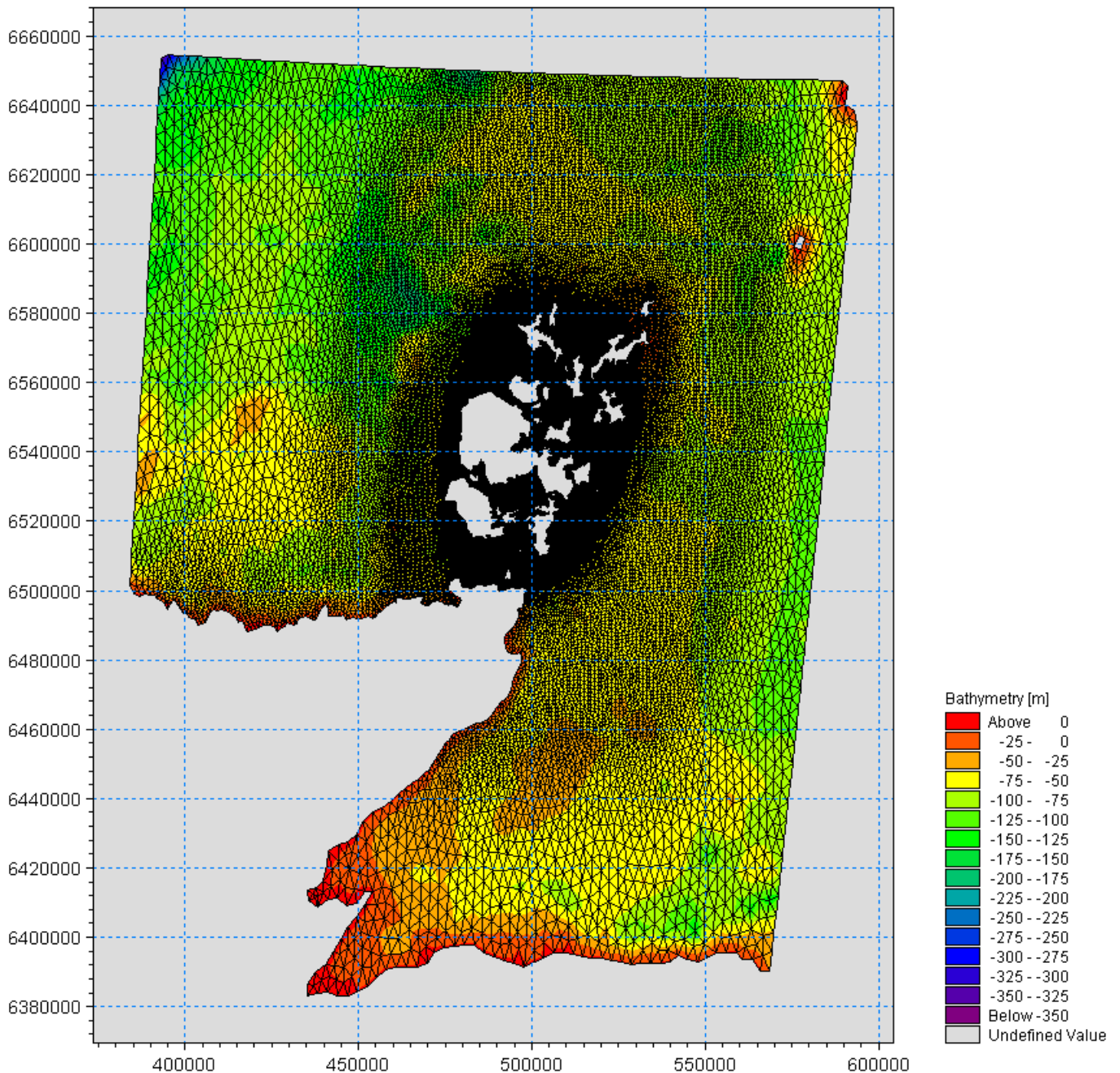


Figure 35 Model mesh grid

Open boundary data was also derived from the FES2004 database. Computational results were obtained taking into account:

- Coriolis force (assuming to be a constant)
- Bottom friction modelled by a Chezy law
- Turbulence viscosity computed with the Smagorinsky model.
- Fixed water depths (minimum water depth 2.5m)

as with the TELEMAC model.

MIKE contains a number of computational options, e.g. high or low order solver in space/time, the inclusion of the tidal potential gravitational forcing, fixed shoreline versus flooding and drying at the shoreline of the model, uniform or varying Coriolis force, bed friction formulations, density variation and others. There are also a number of environmental options such as the inclusion of precipitation, wind forcing, and flow structures such as weirs, piers, tidal turbines and others. However most of these options are outside the scope of the comparison.

The baseline model was also run with a uniform Chezy coefficient of 60. MIKE21 also permits the Chezy coefficient to vary through the domain. MIKE documentation recommends using the alternative bottom friction formulation, which is a Manning's number formulation. This provides a friction value that directly changes with the model depth, unlike the Chezy formulation. The

Manning’s number may also change through the domain, allowing changes in friction that may correspond to bed type for example.

3.4.2 Model Output

An example current map of the flow through Fall of Warness is provided in **Figure 36**. The major flow fields are reproduced.

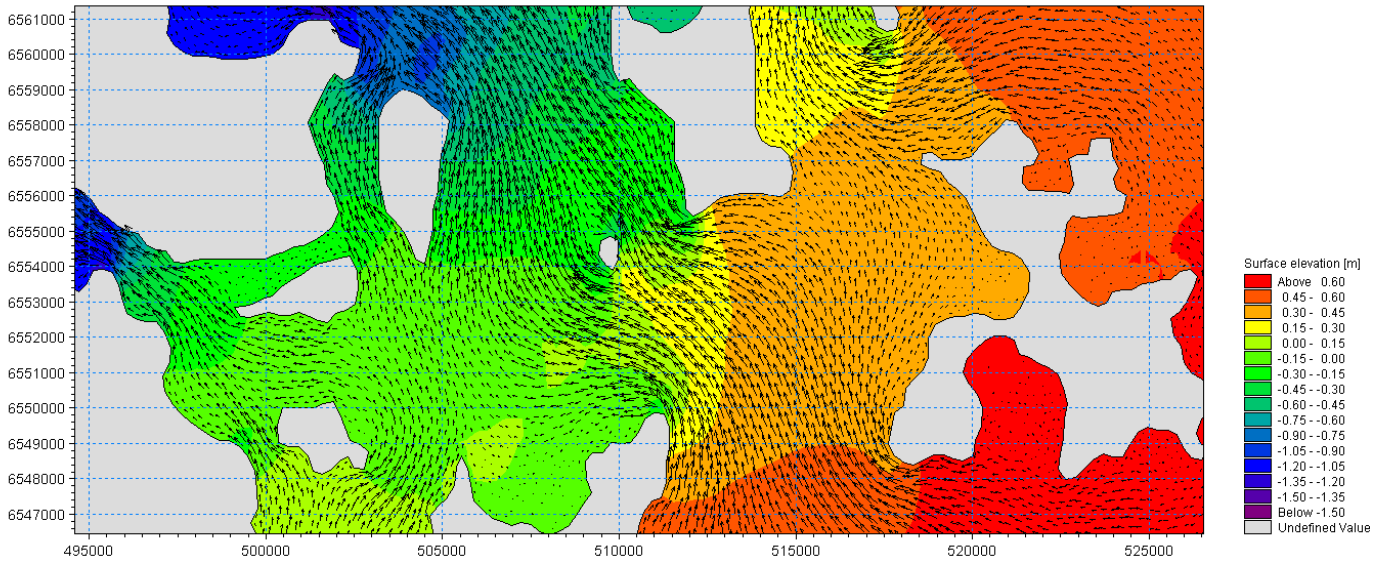


Figure 36 Current map of Fall of Warness – 07/04/2005 HW +3h

- Sea levels

Time series of the predicted and modelled tidal elevations for the port of Wick is shown in Figure 37. The model over predicts slightly during the neap to spring cycle, but under predicts during the sprint to neap. The results agree well with the Telemac results.

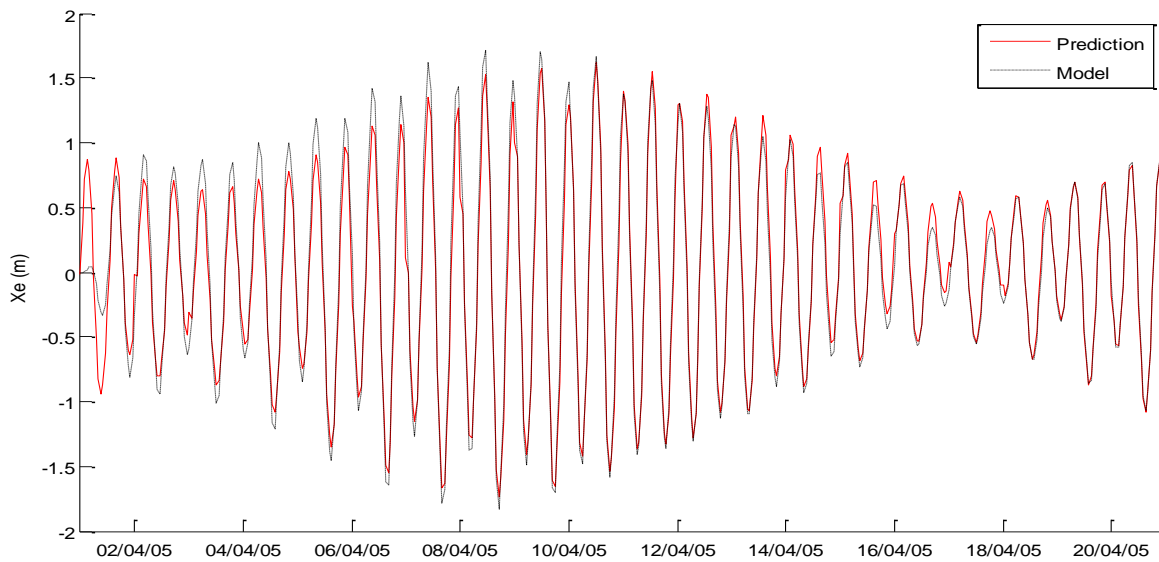


Figure 37 Tidal comparison at Wick

A comparison of the two series is made in Figure 38. The agreement is very close, with very little bias.

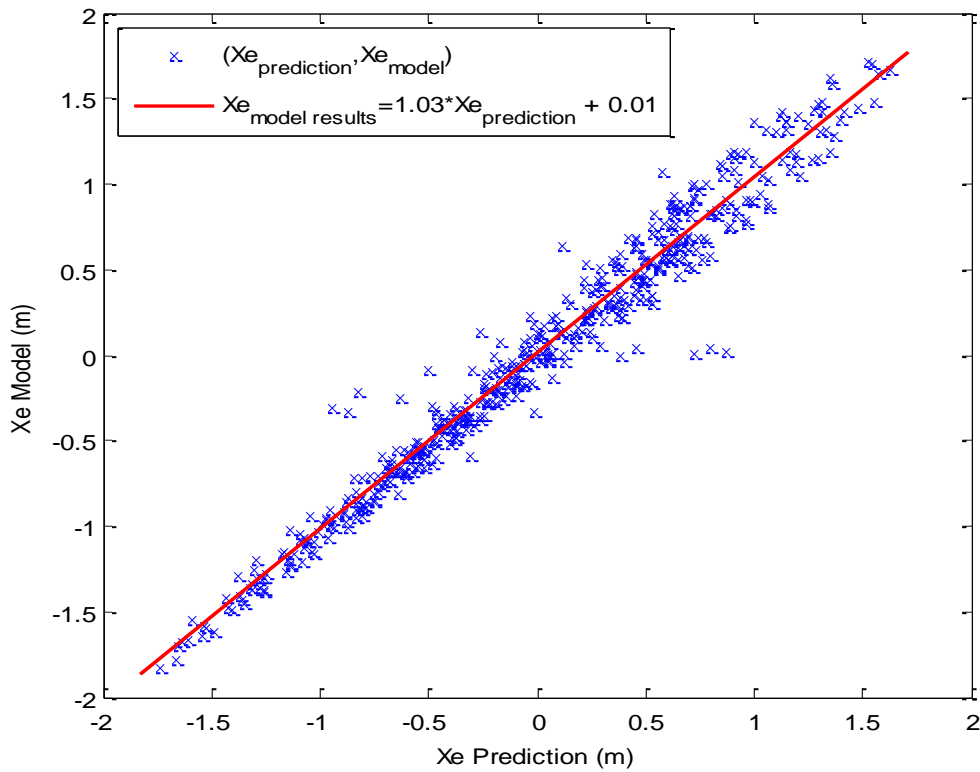


Figure 38 Predicted against modelled sea level at Wick

The time series of observed and modelled elevations for station 7 are shown in Figure 39. Again the general features of the amplitude are well reproduced. There are both underestimated and overestimated peaks.

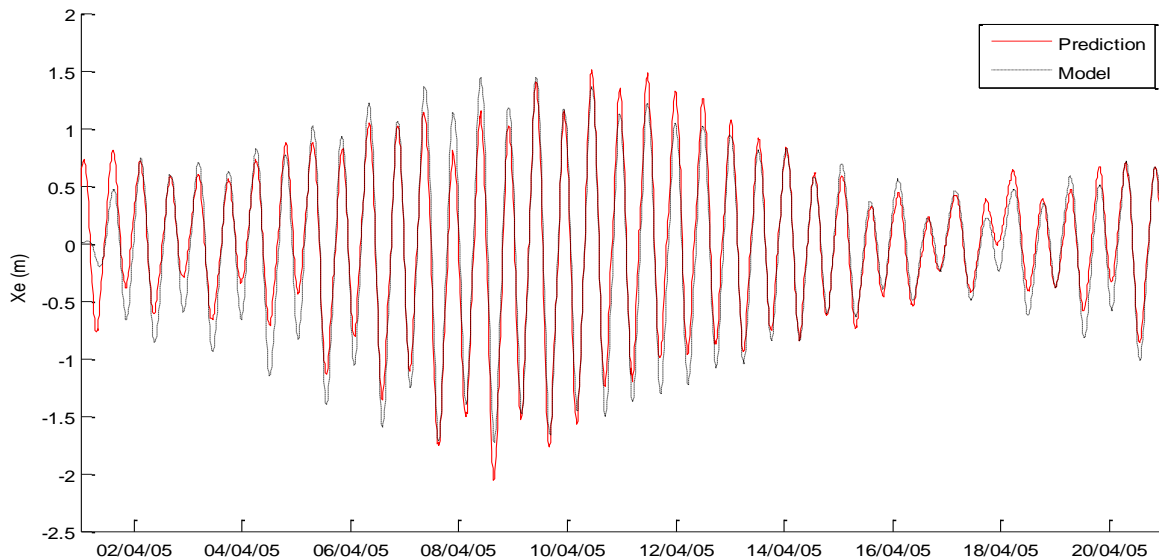


Figure 39 Tidal comparison at Station 7

The elevations are compared in Figure 40. The overall agreement is very high.

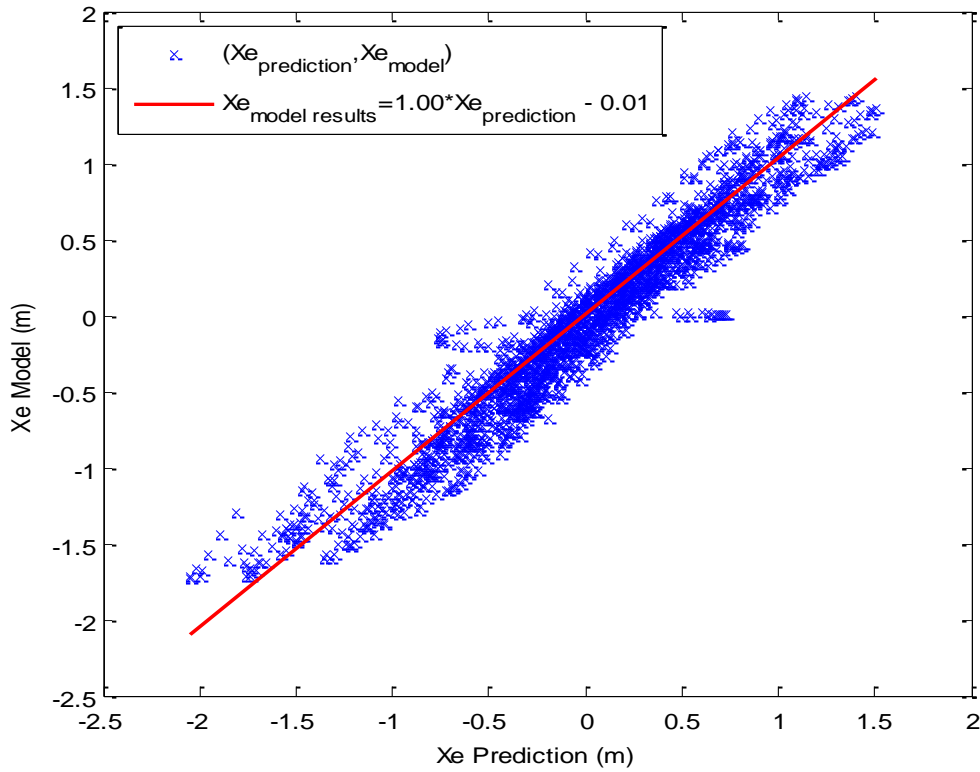


Figure 40 Observed against measured elevations at station 7

- *Currents*

The currents observed and modelled at point 7 are shown in Figure 41. The general features are mostly well reproduced, with some under-estimating of the peak flows. The corresponding directions are shown in Figure 42 and also show good agreement.

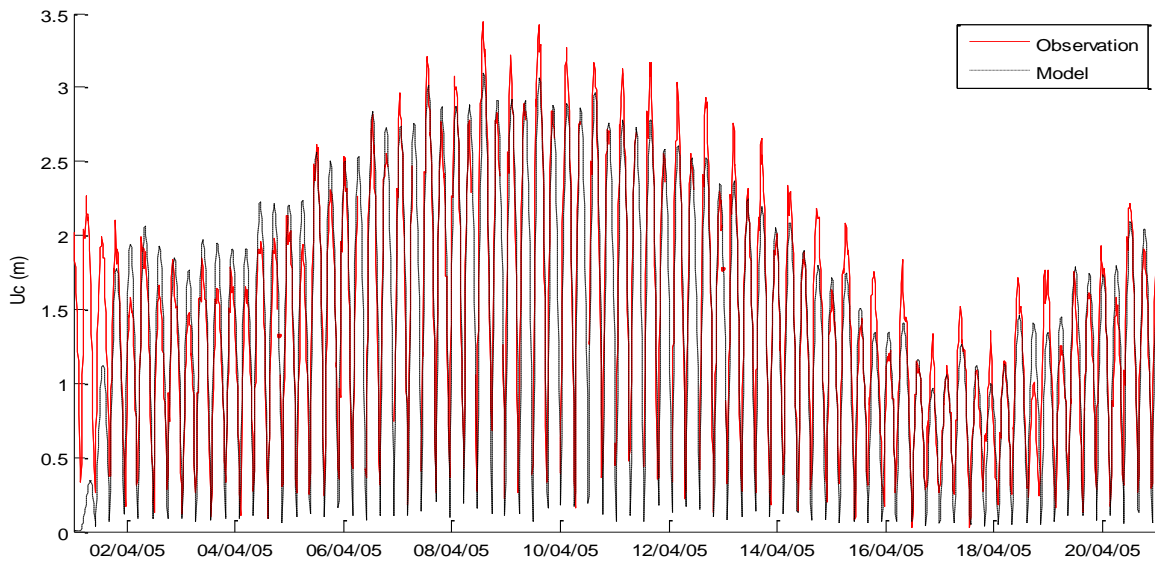


Figure 41 Current comparison at Station 7

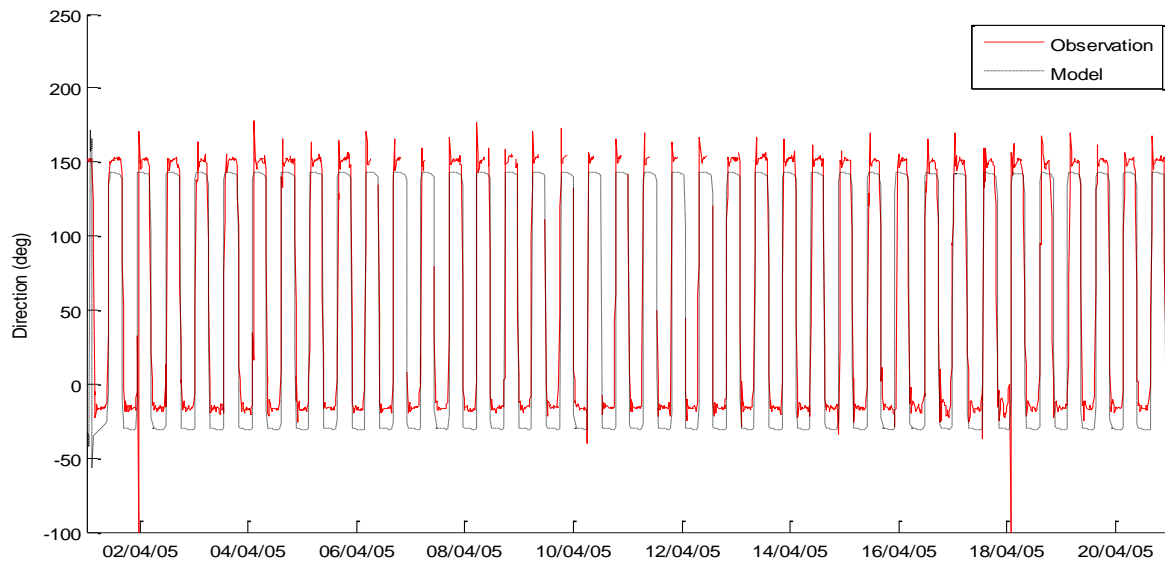


Figure 42 Direction comparison at Station 7

A comparison of the values is shown in Figure 43 showing the closeness of the current magnitude results.

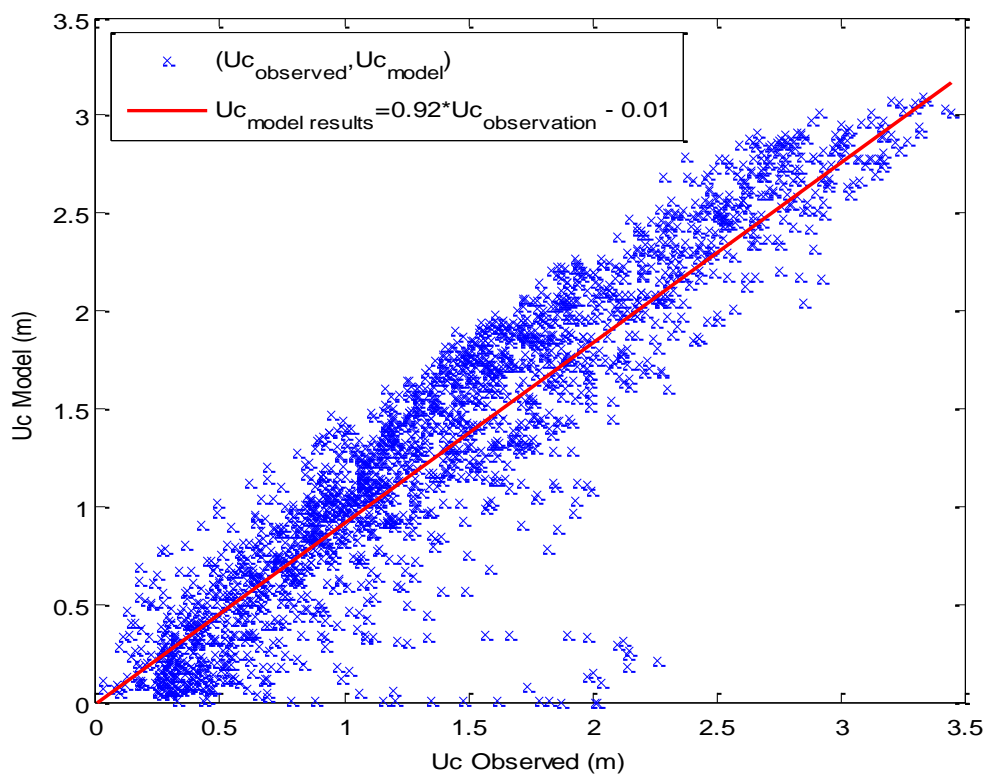


Figure 43 Observed against modelled currents at Station 7

The currents modelled for station 6 are seen in Figure 44, Figure 45 and Figure 46. The underestimating of the currents here is more significant than at station 7, while the directions are in good agreement.

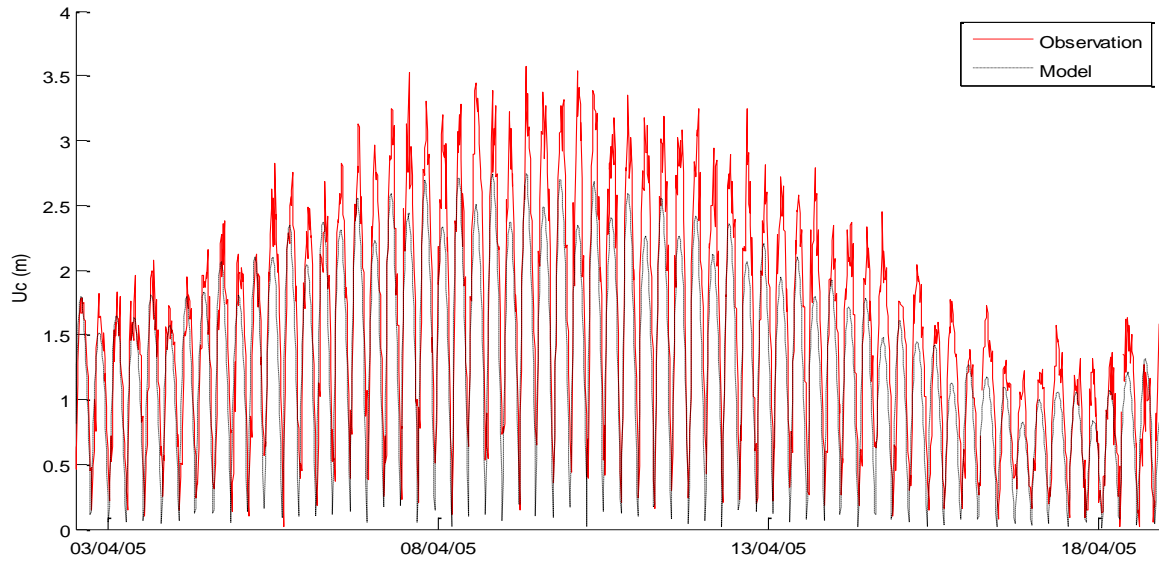


Figure 44 Current comparison at Station 6

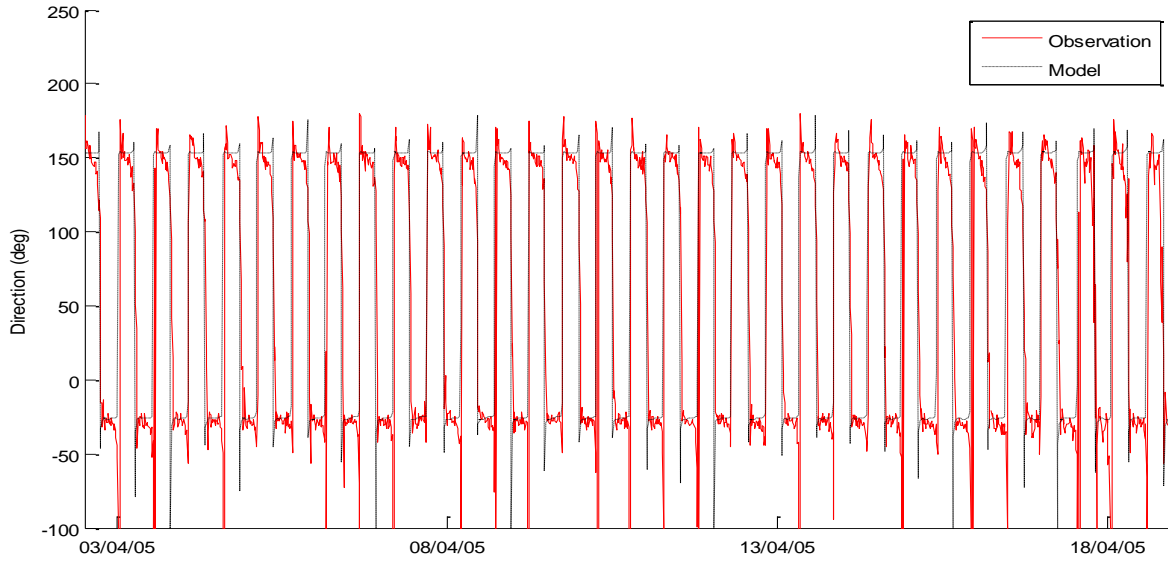


Figure 45 Direction comparison at Station 6

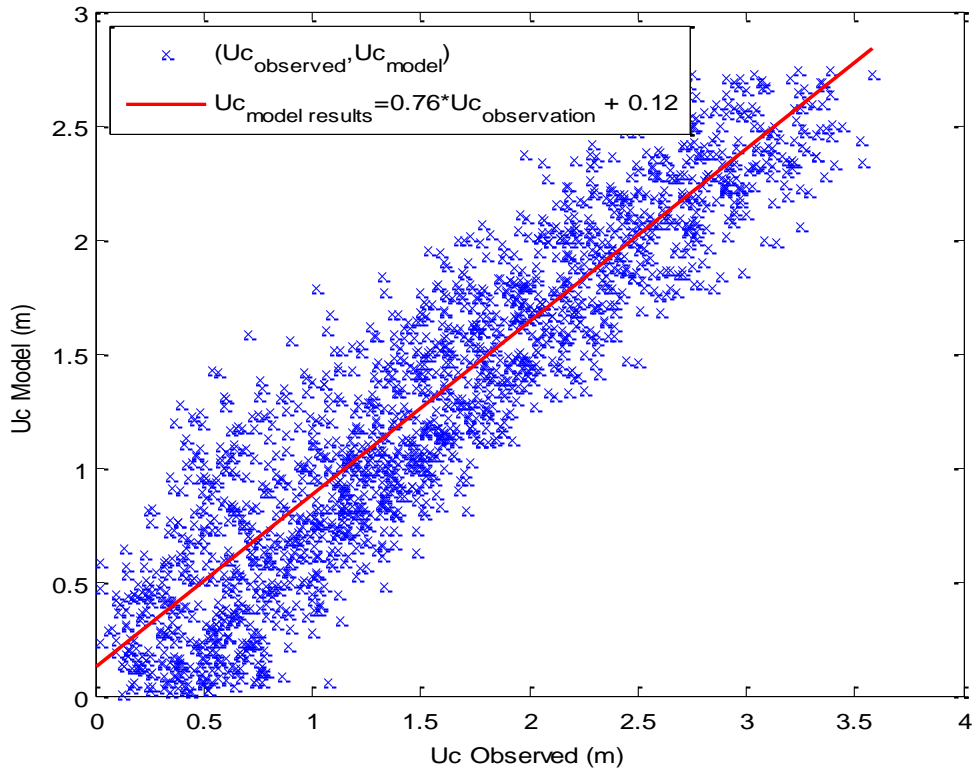


Figure 46 Observed against modelled currents at Station 6

Comparisons of the currents at station 6 for different values of the Chezy coefficient are shown in Figure 47 and Figure 48. The higher damping caused by the lower Chezy coefficient is clear.

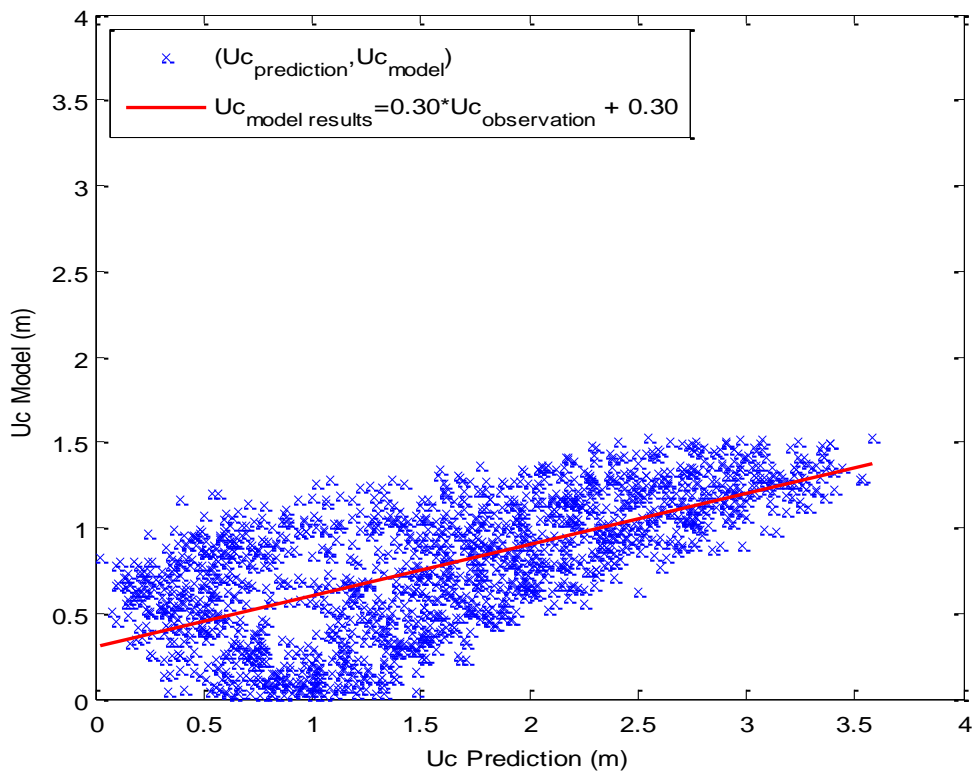


Figure 47 Observed against modelled currents at Station 6 – Chezy coefficient = 30

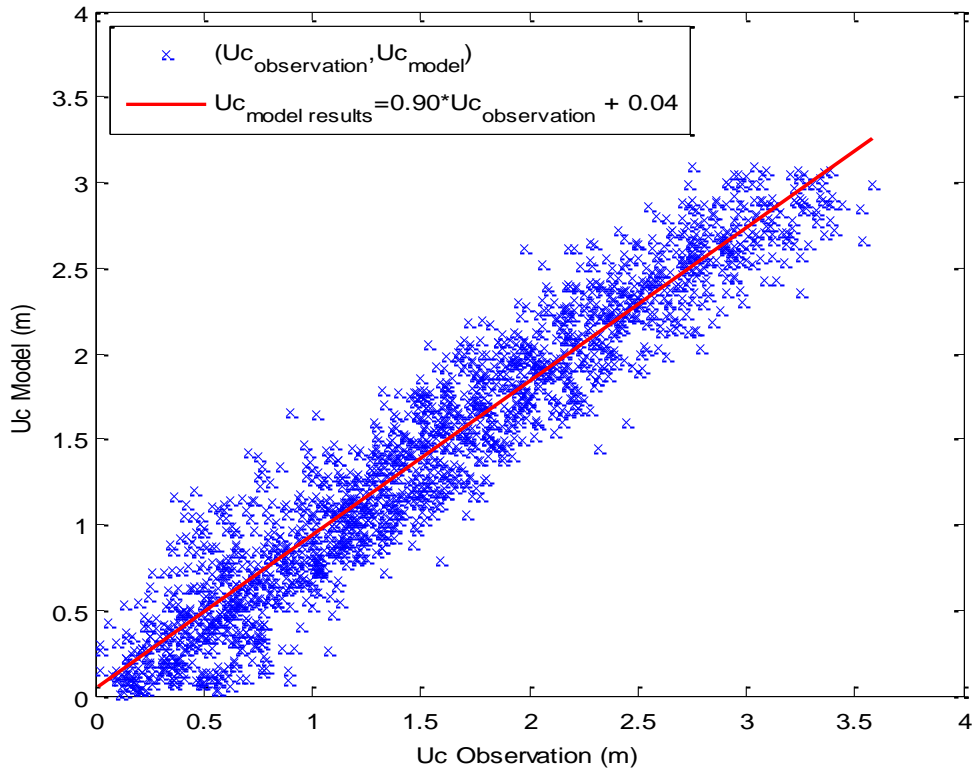


Figure 48 Observed against modelled currents at Station 6 – Chezy coefficient = 80

Samples of the flow field are shown in Figure 49 and Figure 50. The reduced currents corresponding to the lower coefficient are shown.

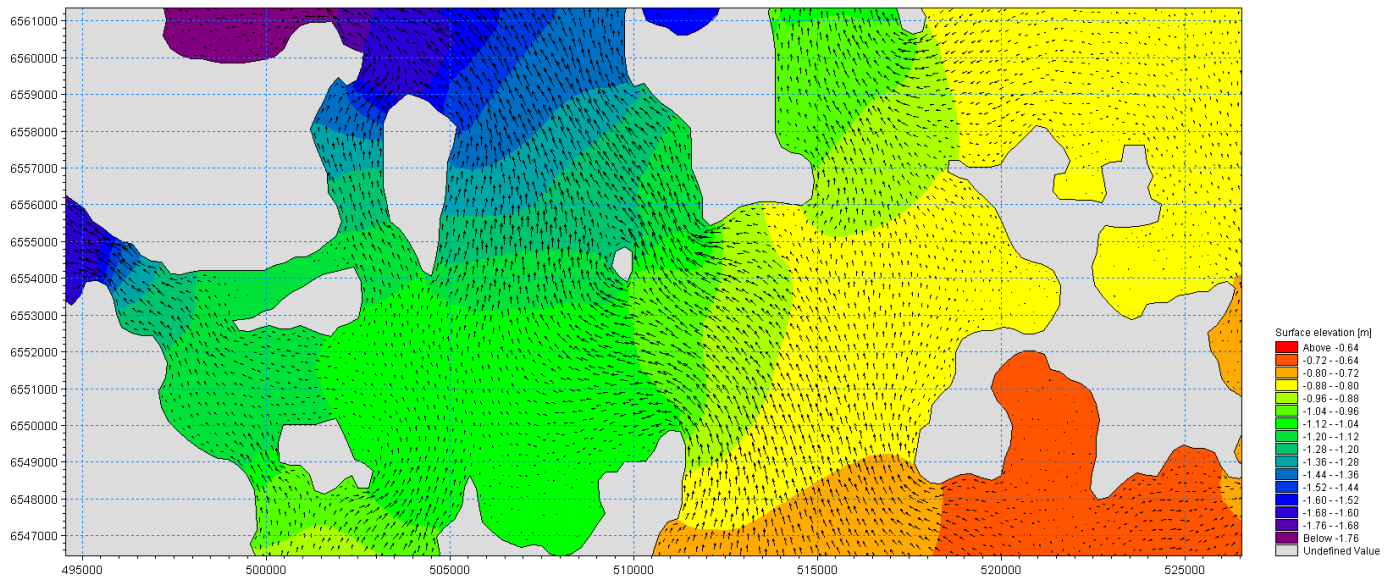


Figure 49 Current map at 06/04/2005 - Chezy coefficient = 30

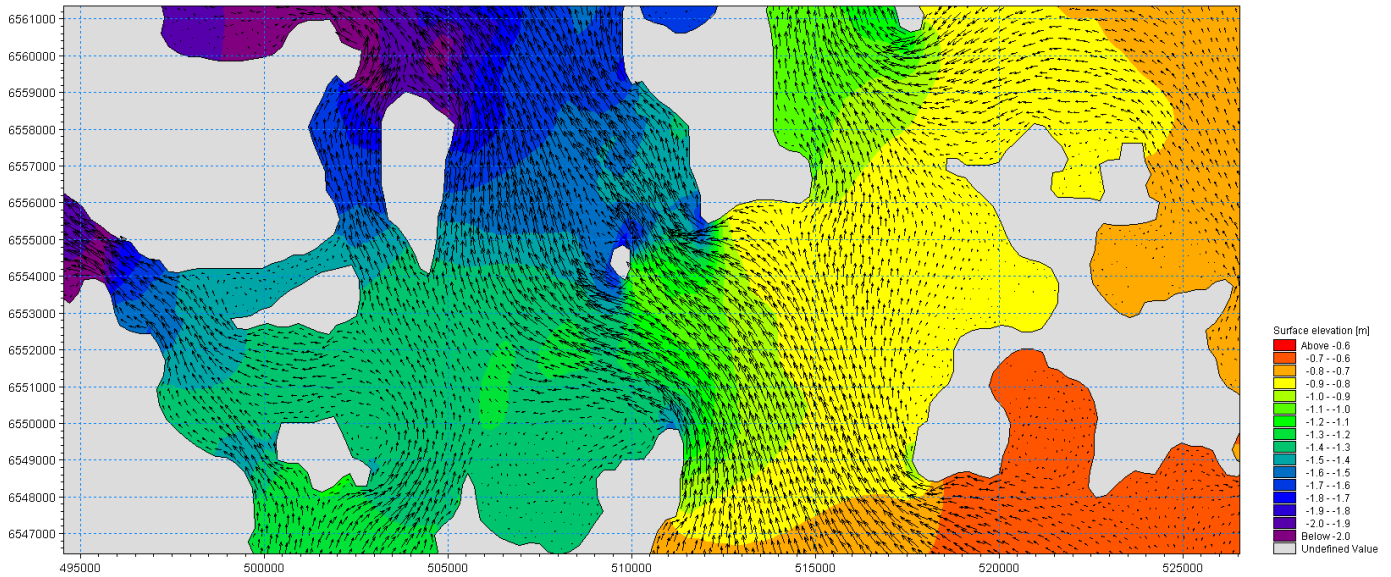


Figure 50 Current map at 06/04/2005 - Chezy coefficient = 70

A comparison run was made using the Manning’s number formulation of bed friction. Current maps are compared below. A uniform Chezy coefficient of 60 is shown in Figure 51 and a uniform Manning’s number of 42 is shown in Figure 52. The higher bed friction in shallow water areas due to the Manning’s formulation can be seen by the reduced current magnitude close to the shoreline. Changes in the overall pattern of surface elevation can also be seen, as the tidal heights are damped differently according to the friction laws chosen.

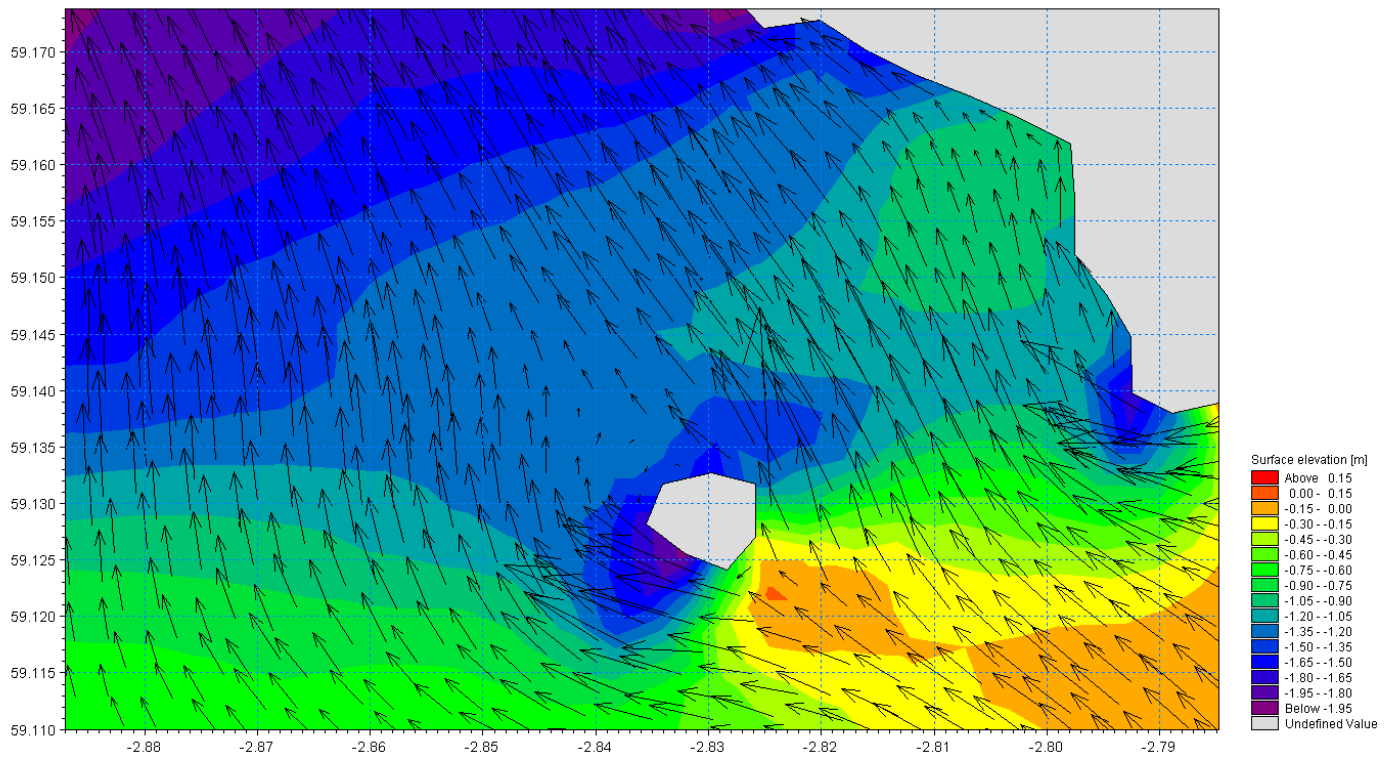


Figure 51 Current map - Chezy coefficient = 60

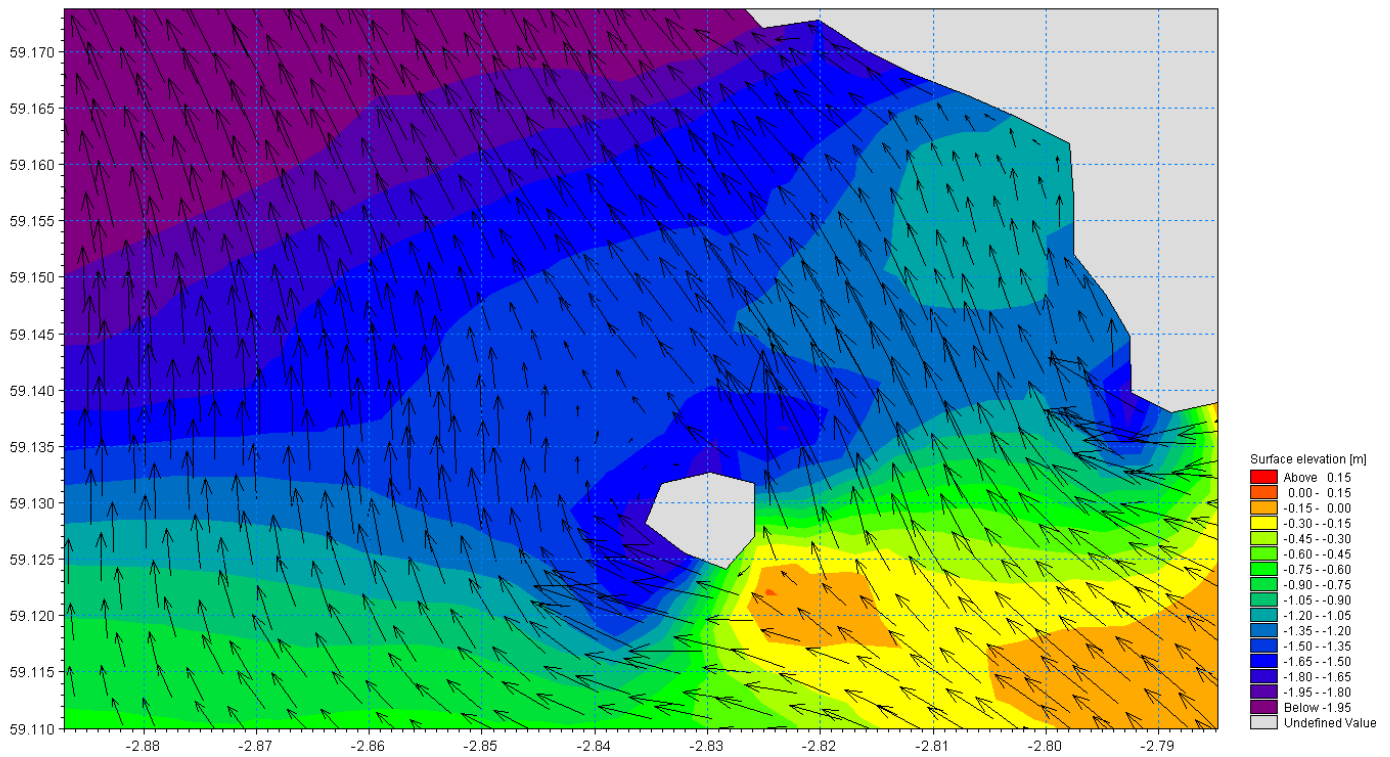


Figure 52 Current map – Manning’s number = 42

The modelled and observed currents for station 7 with the Mannings formulation are shown in Figure 53. This contains a mixture of under and over predictions, generally over-predicting before the spring tide, and under-predicting after the spring tide.

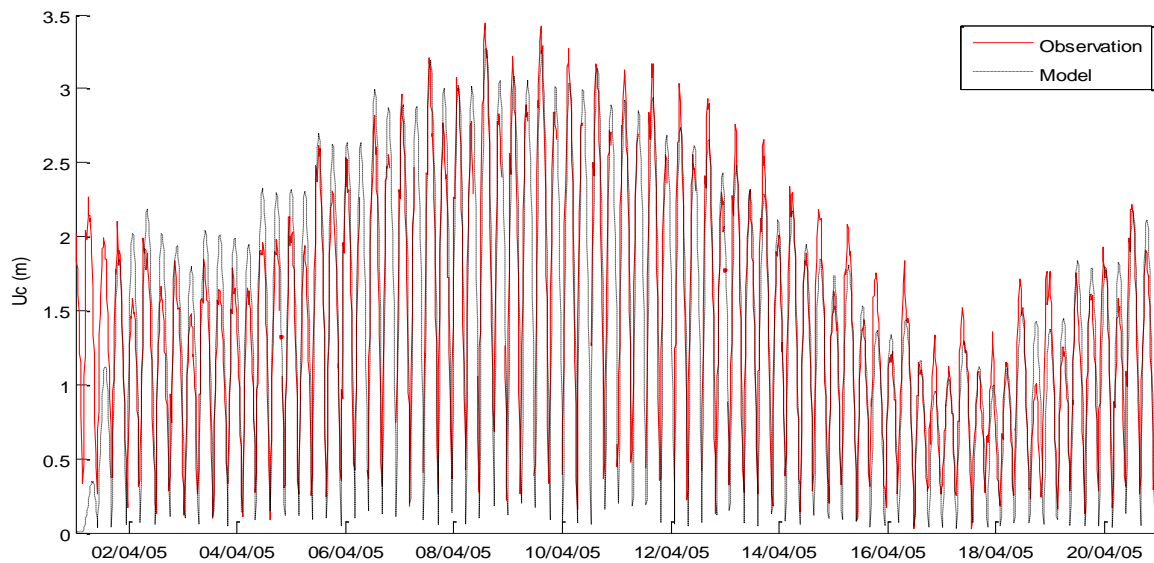


Figure 53 Current comparison Station 7 - Manning’s number = 42

The directions for this case are show in Figure 54 and again show close agreement.

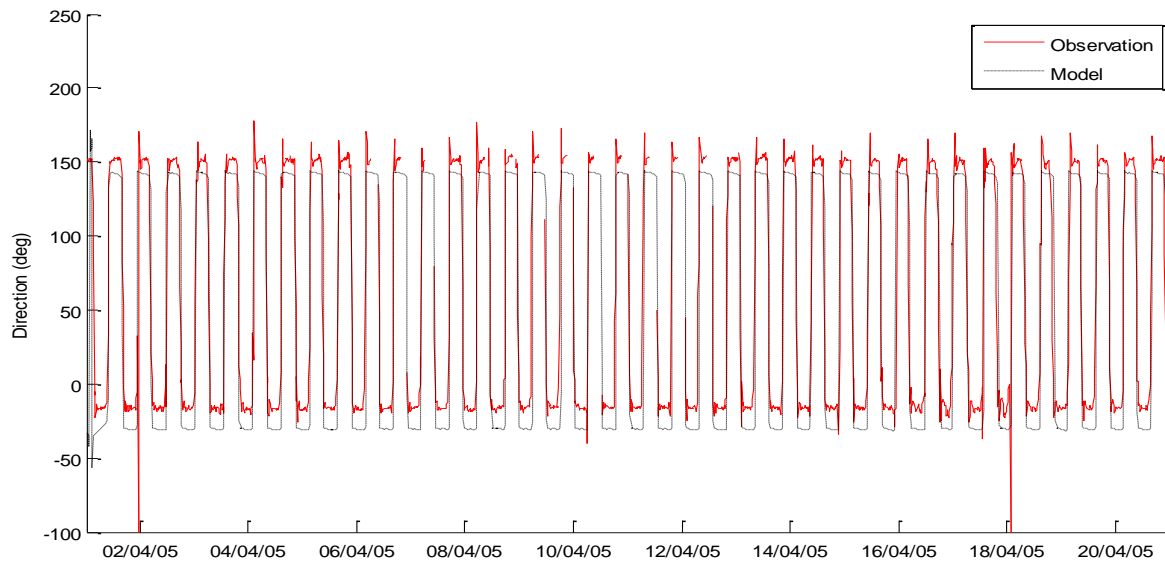


Figure 54 Direction comparison Station 7– Manning’s number = 42

A comparison of the observed and modelled currents is shown in Figure 55, and the overall agreement is very close.

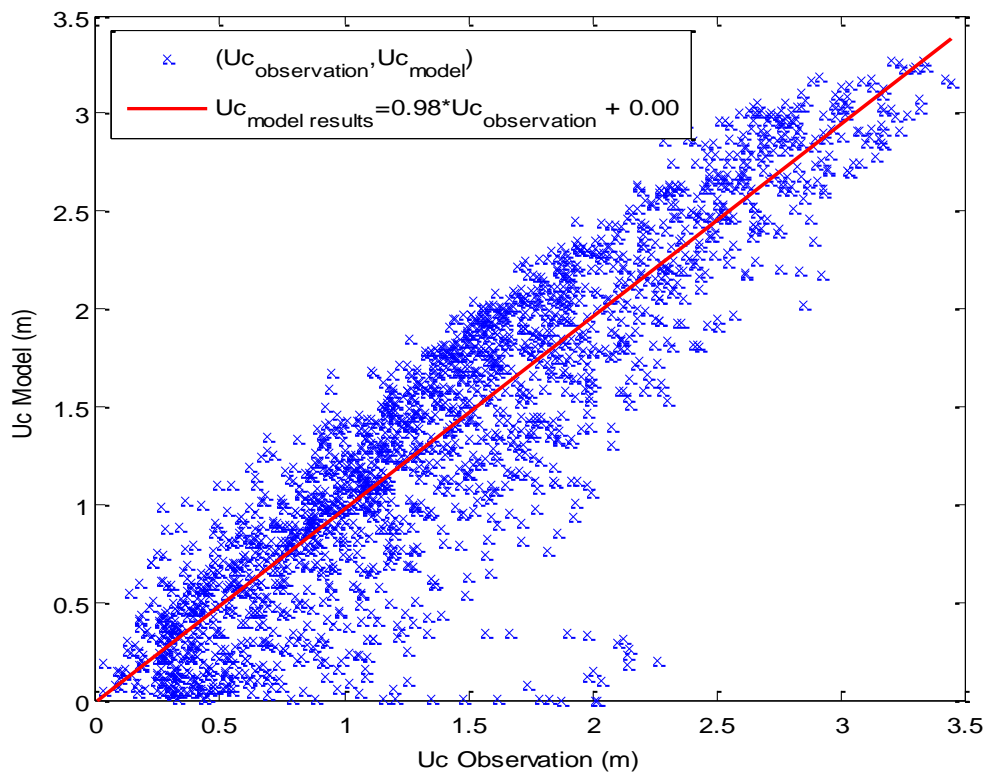


Figure 55 Observed against modelled currents at Station 7 - Manning’s number = 42

Considering station 6, the modelled and observed velocities are shown in Figure 56. A general pattern of under-estimating is seen.

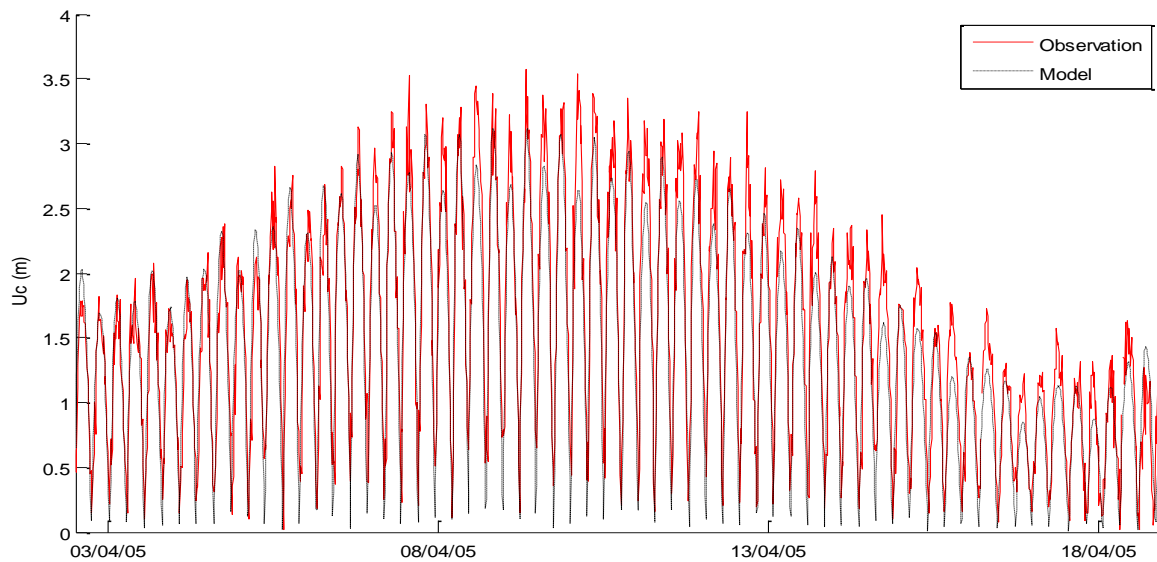


Figure 56 Current comparison at Station 6 - Manning’s number = 42

These are compared in Figure 57, and the overall agreement is high, comparable to the Chezy number=70 case.

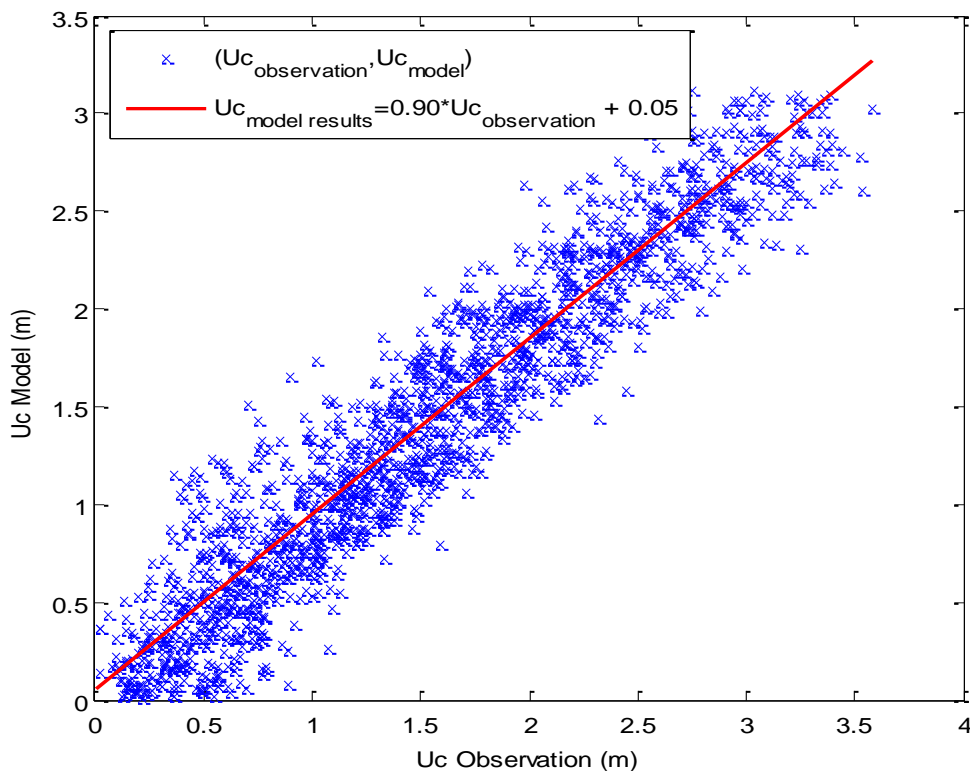


Figure 57 Observed against modelled currents at Station 6 - Manning’s number = 42

Another mode of the MIKE model is the ability to move the shoreline as the surface elevation changes. This is expected to provide better model performance in areas where shallow waters dominates the tidal patterns (e.g. estuarine flows). The Orkney archipelago mostly consists of deeper water, and the largest shallow area is not connected to Fall of Warness. A further run of the model, again with a uniform Chezy coefficient = 60 was performed, and with wetting/drying option enabled. A comparison of the current magnitudes modelled at station 7 for the wetting/drying mode against the fixed depth mode is shown in Figure 58. The differences are mostly negligible, but the largest differences are of the order of 0.15 m/s.

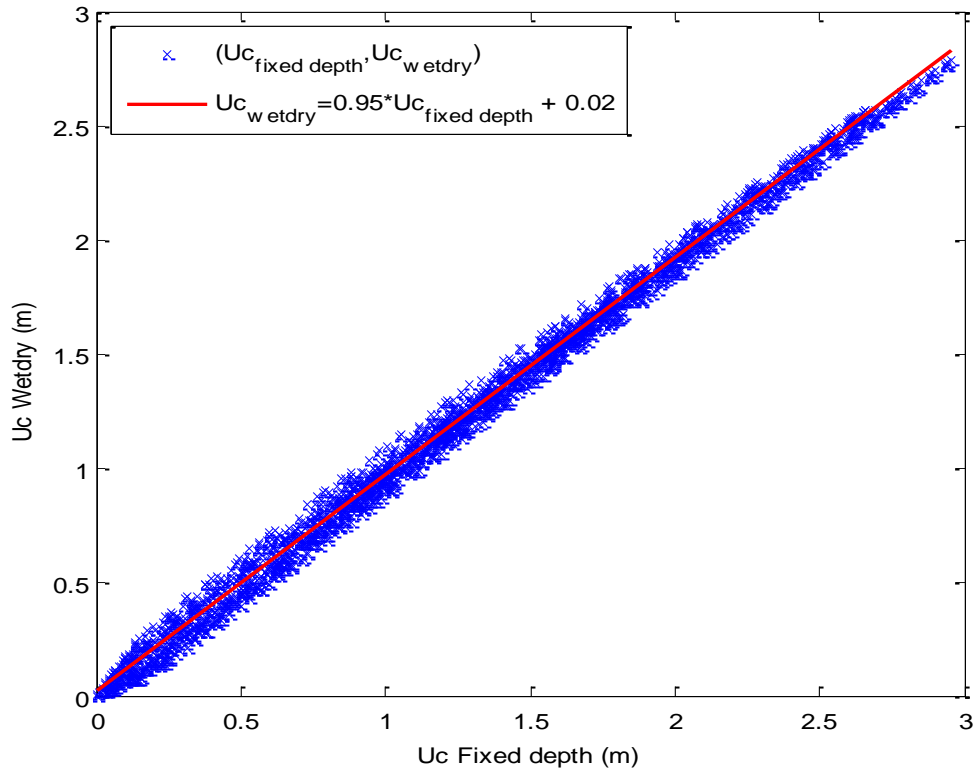


Figure 58 Observed against modelled currents at Station 6 - Manning's number = 42

This result confirms the flow is dominated by the deep water bodies in the area.

4 DISCUSSION

The two hydrodynamic models applied in this report are implemented on a finite element computational grid of triangular elements. This grid enables to adapt the horizontal step using large mesh grid near the border and refined mesh grid at the coast. This is particularly interesting in such rugged coastlines (with many islands) where it could be difficult to implement various nested models. Indeed, open boundaries forcing from the parent to the embedded model can become a hard work in these areas.

The two models are 2 dimension models and they have been implemented on similar grids, using the same bathymetry and the same open boundaries conditions. This has resulted in very similar estimations of tidal currents and sea levels.

Both studies have highlighted the possibility to adjust bottom friction, for example by changing the Chezy coefficient or the Manning formulation, in order to improve sea level and/or current prediction. Here, current measurements are only available on few points all positioned in the same area and the friction coefficients are, therefore, homogeneous through the domain. However, in the two models it is possible, if necessary, to vary the coefficient over the domain to get a better spatial adjustment.

In some areas, it will be necessary to take into account meteorological conditions to better estimate currents and sea levels. Depending on the model it is possible, and relatively straightforward, to model the influence of atmospheric pressure and/or wind stress. Atmospheric forcing can change in time and/or space or remain homogeneous and constant. In the Telemac model it is easily possible to take into account homogeneous and constant winds. It is also possible to force the model with variable winds but it requires further developments. The MIKE series of models has similar capability not utilised here. A very important aspect, when trying to model meteorological effects regardless of the different models capabilities, is to implement it on a large enough domain.

Where areas of shallow water have influence, correct modelling of the shoreline is needed with a suitable 'wetting/drying' approach. This allows the volume of water under consideration to change appropriately. Application of such an algorithm requires careful treatment of shallow/drying thresholds.

The keystone to obtaining satisfying results, with 2D hydrodynamic models in particular, is the bathymetry. The bathymetry should be accurate enough to propagate correctly the tidal wave from the open boundaries to the coast, and its spatial resolution should be high enough at the coast to enable a satisfying mesh grid refinement of the studying area. The location of Orkney is very complex and the coarse bathymetry results shown here are only indicative. Finer resolution is required for operational results in this area. These results also show that the implementation of dissipation mechanisms (bed friction/eddy viscosity) is important, and appropriate parameterisations of these mechanisms should be chosen in a given model.